Proton Structure

with Malcolm John

The static quark model, built around loose symmetry principles, successfully describes many patterns in mesons and baryons. The natural question is thus posed: can quarks be "seen" and what of the strong force that holds them together? This question is tackled by scattering high energy probe particles off hadrons. The result is a deep understanding of the dynamics inside the proton, which has proven vital to the design and analysis of high energy hadron colliders.

1 Relativistic scattering

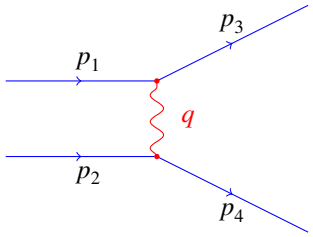
In the *Relativistic Kinematics* notes, there is a derivation of cross section for point-particle scattering in the lab frame,

$$\frac{d\sigma}{d\Omega} = \frac{1}{64\pi^2}|\mathcal{M}_{fi}|^2 \frac{1}{(M + E_1(1-\cos\theta))^2}\,, \tag{1}$$

where M is mass of the target, E_1 is the energy of the probe and θ is the angle of recoil.

For experimental results, a matrix element must be calculated from the Feynman rules for QED scattering of two spin-half point particles. The probe and target particles have initial state 4-momenta p_1 and p_2 and go to final states p_3 and p_4 respectively after the transfer of q.

- The fermions spinors $u(p_1)$ going to $\bar{u}(p_3)$ and $u(p_2)$ going to $\bar{u}(p_4)$.
- From each vertex comes a vertex factor, $ig_e\gamma^\mu$, where $g_e = \sqrt{4\pi\alpha_{\text{EM}}}$.
- The photon propagator give a factor, $\frac{-ig_{\mu\nu}}{q^2}$.
- Integrate over all q but imposing energy and momentum conservation with an appropriate delta function.



This recipe gives a matrix element, $-i\mathcal{M}_{fi}$ developed earlier in the context of $e^+e^- \to \mu^+\mu^-$ scattering but is, in principle, equally valid for scattering of other spin-half particles (read: proton in this context).

$$-i\mathcal{M}_{fi} = \int \left[\bar{u}(p_3)\, ig_e\gamma^\mu\, u(p_1)\right] \frac{-ig_{\mu\nu}}{q^2} \left[\bar{u}(p_4)\, ig_e\gamma^\nu\, u(p_2)\right] \delta^4(p_1 - p_3 - q)\, d^4q\,. \tag{2}$$

$$\mathcal{M}_{fi} = -\frac{g_e^2}{(p_1-p_3)^2} \underbrace{\left[\bar{u}(p_3)\,\gamma^\mu\, u(p_1)\right]}_{j_e^\mu} \underbrace{\left[\bar{u}(p_4)\,\gamma_\mu\, u(p_2)\right]}_{j_{p\mu}} \tag{3}$$

: electron and proton Dirac currents. (4)

The fermion spinors are each have four elements and the γ^μ are 4×4 matrices. In the majority of cases, we are dealing with the scattering of unpolarised particles, this is, the particles have not specific spin direction. This means that we are interested in a spin-average matrix element squared, $\langle|\mathcal{M}_{fi}|^2\rangle$, which can be shown by multiplying-out and summing over

repeated indices, to be

$$\langle|\mathcal{M}_{fi}|^2\rangle = \frac{8g_e^4}{(p_1-p_3)^4}\left[(p_1\cdot p_2)(p_3\cdot p_4)+(p_1\cdot p_4)(p_2\cdot p_3)-m^2(p_2\cdot p_4)-M^2(p_1\cdot p_3)+2m^2M^2\right]. \tag{5}$$

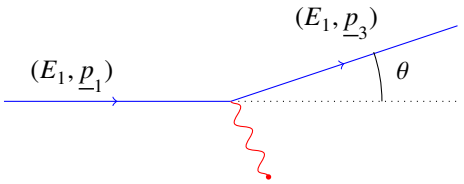
1.1 Mott scattering

Consider the case of an electron (m), scattering off a proton of mass M. In a first example with "low" (but relativistic) probe energy, we neglect the recoil ($\theta = 0$ in Eq. 1). Continuing with the spin-averaged matrix element,

$$\frac{d\sigma}{d\Omega} = \frac{\langle|\mathcal{M}_{fi}|^2\rangle}{(8\pi M)^2}. \tag{6}$$

As the recoil is neglected, the various scalar products are simplified,

$$p_2 = p_4 = (M,0) \qquad p_1 = \left(E_1, \underline{p}_1\right) \qquad p_3 = \left(E_1, \underline{p}_3\right) \qquad |\underline{p}_1| = |\underline{p}_3|.$$



Point particle, negligible recoil. $p_2 = p_4 = (M,0)$

$$(p_1-p_3)^2 = (0, \underline{p}_1-\underline{p}_3)^2 = -|\underline{p}_1|^2 - |\underline{p}_3|^2 + 2\underline{p}_1\cdot\underline{p}_3 = -2|\underline{p}_1|^2(1-\cos\theta) = -4|\underline{p}_1|^2\sin^2\frac{\theta}{2}$$

$$(p_1\cdot p_3) = E_1^2 - \underline{p}_1\cdot\underline{p}_3 = |\underline{p}_1|^2 + m^2 - |\underline{p}_1|^2\cos\theta = m^2 + 2|\underline{p}_1|^2\sin^2\frac{\theta}{2}$$

$$(p_1\cdot p_2)(p_3\cdot p_4) = (p_1\cdot p_4)(p_2\cdot p_3) = M^2E_1^2 \quad \text{and} \quad (p_2\cdot p_4) = M^2.$$

Putting this into Eq. 5, then Eq. 6,

$$\frac{d\sigma}{d\Omega} = \frac{1}{(8\pi M)^2}\frac{8g_e^4}{(-4|\underline{p}_1|^2\sin^2\frac{\theta}{2})^2}\left[2M^2E_1^2 - m^2M^2 - M^2\left(m^2+2|\underline{p}_1|^2\sin^2\tfrac{\theta}{2}\right)+2m^2M^2\right]$$

With $g_e = \sqrt{4\pi\alpha}$, the scattering formula is,

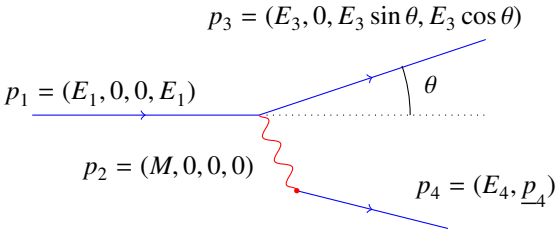
$$\frac{d\sigma}{d\Omega} = \left(\frac{\alpha}{2|\underline{p}_1|^2\sin^2\frac{\theta}{2}}\right)^2\left[m^2 + |\underline{p}_1|^2\cos^2\tfrac{\theta}{2}\right]. \tag{7}$$

Such a scattering cross section is relevant for relativistic electrons ($m = 0.511\,\mathrm{MeV}/c^2$) with energies $O(1-10\,\mathrm{MeV})$, well below the proton mass ($M = 938\,\mathrm{MeV}/c^2$). The non-relativistic limit, the probe has momentum $|\underline{p}_1|^2 \ll m^2$ the second term can be neglected. Using kinetic energy $E_K = p^2/2m$, the Rutherford scattering cross (for $Z = 1$) section is recovered,

$$\frac{d\sigma}{d\Omega} = \frac{\alpha^2}{16\,E_K^2\,\sin^4\frac{\theta}{2}}.$$

$e^- \to p^+$ scattering with recoil

At slightly higher energy, we include recoil but can neglect the probe mass, $E_1 \gg m$. As energy is passed to the proton, the electron changes energy as well as direction. With $m = 0$ and the proton (of mass M) initially at rest the fourvectors are,



From Eq. 5 for $m = 0$,

$$\langle|\mathcal{M}_{fi}|^2\rangle = \frac{8g_e^4}{(p_1 - p_3)^4}\left[(p_1\cdot p_2)(p_3\cdot p_4) + (p_1\cdot p_4)(p_2\cdot p_3) - M^2(p_1\cdot p_3)\right].$$

$$\text{with} \quad p_1\cdot p_2 = E_1 M \qquad p_1\cdot p_3 = E_1E_3(1-\cos\theta) \qquad p_2\cdot p_3 = E_3 M\,.$$

And $(p_1 - p_3)^4$ comes from,

$$\begin{aligned} q^2 = (p_1 - p_3)^2 &= \cancel{p_1^2} + \cancel{p_3^2} - 2p_1\cdot p_3 = -2\,(E_1E_3 - E_1E_3\cos\theta) \\ &= -4E_1E_3\sin^2\tfrac{\theta}{2}. \end{aligned}$$

The fourmomentum-squared is negative.
Use momentum conservation to side-step using the unmeasured proton recoil, $p_4 = p_1 + p_2 - p_3$ in the following,

$$\begin{aligned} p_3\cdot p_4 = &\qquad p_3\cdot p_1 + p_3\cdot p_2 - p_3\cdot p_3 \\ &= E_1E_3(1-\cos\theta) + \;E_3M\; - \;\cancel{m^2} \end{aligned}$$

$$\begin{aligned} p_1\cdot p_4 &= p_1\cdot p_1 + p_1\cdot p_2 - p_1\cdot p_3 \\ &= \;\cancel{m^2}\; + \;E_1M\; - E_1E_3(1-\cos\theta) \end{aligned}$$

So, $$\langle|\mathcal{M}_{fi}|^2\rangle = \frac{8g_e^4}{16E_1^2E_3^2\sin^4\frac{\theta}{2}}\left[(E_1M)\,(E_1E_3(1-\cos\theta) + E_3M) + (E_1M - E_1E_3(1-\cos\theta))\,(E_3M)) - M^2\,(E_1E_3(1-\cos\theta))\right],$$

$$\begin{aligned} \langle|\mathcal{M}_{fi}|^2\rangle &= \frac{8g_e^4}{16E_1^2E_3^2\sin^4\frac{\theta}{2}}\,E_1E_3M\left[(E_1 - E_3)(1-\cos\theta) + M(1+\cos\theta)\right], \\ &= \frac{8g_e^4}{16E_1^2E_3^2\sin^4\frac{\theta}{2}}\,2E_1E_3M\left[M\cos^2\tfrac{\theta}{2} + (E_1 - E_3)\sin^2\tfrac{\theta}{2}\right], \end{aligned}$$

The second term is proportional to the energy transferred to the proton, $\nu = E_1 - E_3 \neq 0$. It is dependent on $\sin^2(\theta/2)$ and is associated with the spin-spin ("magnetic") interaction of the two spin-$\frac{1}{2}$ particles. An expression for ν can be derived using conservation of proton fourmomentum,

$$\begin{aligned} q + p_2 = p_4 \quad \Rightarrow \quad q^2 + p_2^2 + 2q\cdot p_2 &= p_4^2 \\ q^2 + \cancel{M^2} + 2q\cdot p_2 &= \cancel{M^2} \\ q^2 &= -2(p_1 - p_3)\cdot p_2 \\ q^2 &= -2(E_1 - E_3)\cdot M \qquad (m \approx 0) \\ E_1 - E_3 \;&=\; -\frac{q^2}{2M} \end{aligned}$$

Note that two independent expressions for q^2 have been derived for the elastic scatter,

1. $q^2 = -2E_1E_3\,(1-\cos\theta)$ conserves the fourmomentum of the electron.
2. $q^2 = -2M(E_1 - E_3)$ conserves fourmomentum of the recoiling, intact proton.

Equating these expressions shows how the electron energy after the scatter and the fourmomentum transfer into the proton are both calculable from the scattering angle alone, assuming the electron beam energy is well defined (always is).

$$E_3 = \frac{ME_1}{M + E_1(1-\cos\theta)} \qquad q^2 = -\frac{2ME_1^2(1-\cos\theta)}{M + E_1(1-\cos\theta)} \tag{8}$$

Altogether the spin-averaged matrix element squared is,

$$\langle|\mathcal{M}_{fi}|^2\rangle = \frac{g_e^4 M^2}{E_1E_3\sin^4\frac{\theta}{2}}\left[\cos^2\tfrac{\theta}{2} - \frac{q^2}{2M^2}\sin^2\tfrac{\theta}{2}\right].$$

Then again using the standard phase-space result of Eq. 1 with Eq. 8(a) plugged in,

$$\frac{d\sigma}{d\Omega} = \frac{1}{64\pi^2}\left(\frac{E_3}{E_1M}\right)^2\langle|\mathcal{M}_{fi}|^2\rangle$$

we arrive at the Mott Scattering formula for relativistic e^- scattering off a recoiling point particle,

$$\left(\frac{d\sigma}{d\Omega}\right)_{\text{Mott}} = \left(\frac{E_3}{E_1}\right)\frac{\alpha^2}{4E_1^2\sin^4\frac{\theta}{2}}\left[\cos^2\tfrac{\theta}{2} - \frac{q^2}{2M^2}\sin^2\tfrac{\theta}{2}\right] \tag{9}$$

Phys. Rev. 102(3) (1956) *"Elastic scattering of 188-MeV electrons"*

This paper shows early work (by 1961 Nobel Prize winner, Robert Hofstadter) electron-nucleon scattering using 100 MeV electrons. The experimental setup is simple, a spectrometer to measure momentum ($\approx E$ for relativistic electrons)

The energy vs. scattering angle relationship of Eq. 8 is seen in the data (below left).

The deviation from Mott scattering in the cross-section vs. scattering angle (below right) is visible at these probe energies. Historically labelled "anomalous", this was the first evidence that the proton was not a point particle.

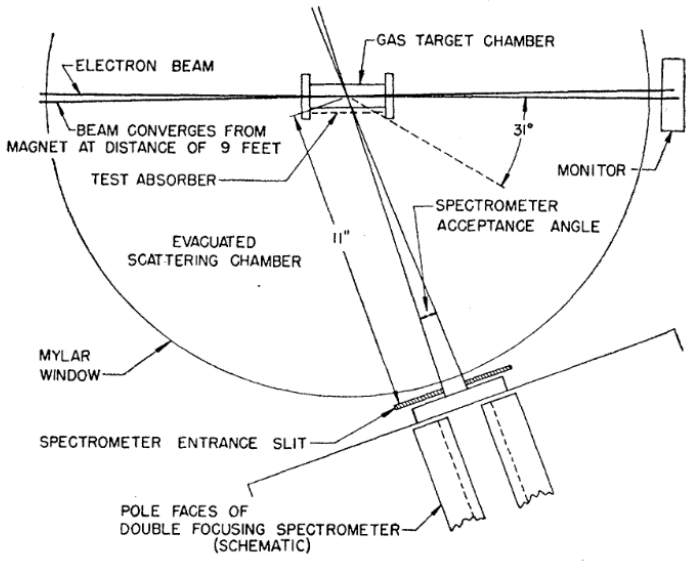
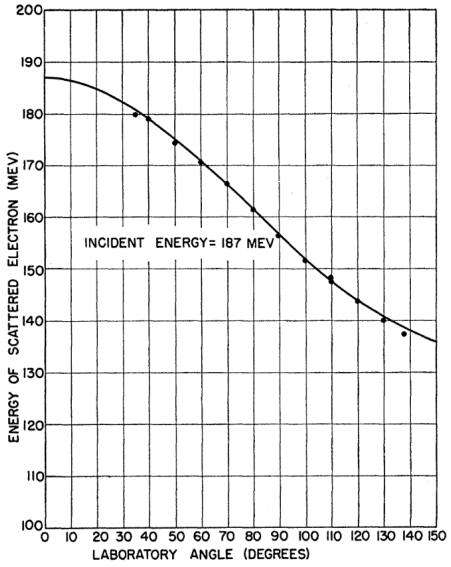
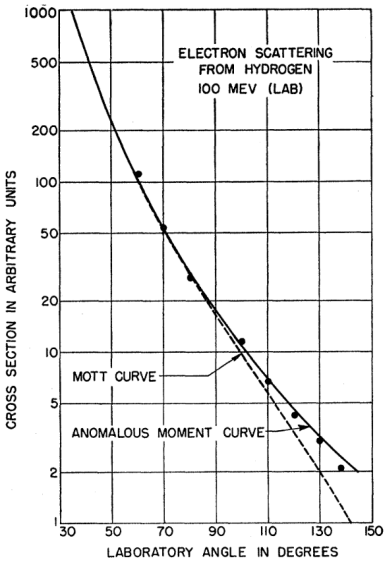


FIG. 2. Arrangement of parts in experiments on electron scattering from a gas target.



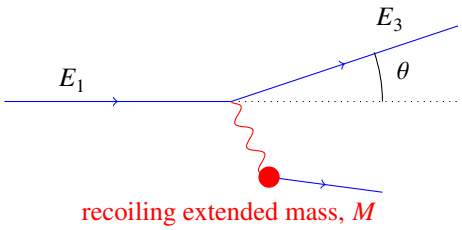


1.2 The Rosenbluth equation

The anomalous moment motivates the inclusion of a form factor $F(q^2)$ in the differential cross section of the proton,

$$\frac{d\sigma}{d\Omega} = \left(\frac{d\sigma}{d\Omega}\right)_{\text{Mott}} \left|F(q^2)\right|^2 ,$$

where F(0)=1 is the low energy case where the proton appears point-like. For higher probe energies, the de Broglie wavelength of the electron is such that it scatters off the internal structure of the proton and $F(q^2) < 1$.



The proton current in the matrix element is modified to include two form factors,

$$j^\mu = \bar{u}(p_4)\,\gamma_\mu\,u(p_2) \quad \Rightarrow \quad j_p^\mu = \bar{u}(p_4)\left[\ \gamma_\mu F_1(q^2) \ + \ \frac{i\kappa_p}{2M}F_2(q^2)\sigma^{\mu\nu}q_\nu\ \right]u(p_2)$$

Dirac point charge — extended Dirac charge — anomalous moment

where $\kappa_p = 1.79$ is the anomalous magnetic moment of the proton,

$$\mu_p = \frac{(1+\kappa_p)e}{2M}\hbar \qquad\qquad c.f.\ \text{Bohr magneton: } \mu_B = \frac{e}{2m_e}\hbar$$

Using this form of the proton current the differential cross section evolves (not proved here) from Eq. 9 to,

$$\frac{d\sigma}{d\Omega} = \left(\frac{E_3}{E_1}\right)\frac{\alpha^2}{4E_1^2\sin^4\frac{\theta}{2}}\left[\left(F_1^2 - \frac{\kappa_p^2 q^2}{4M^2}F_2^2\right)\cos^2\tfrac{\theta}{2} - \frac{q^2}{2M^2}\left(F_1+\kappa_p F_2\right)^2\sin^2\tfrac{\theta}{2}\right], \tag{10}$$

where the new terms are highlighted. Mott scattering, which treats the proton as a point-like, spin-$\frac{1}{2}$ Dirac particle, has $\kappa_p = 0$ and $F_1(q^2) = F_2(q^2) = 1$.[1] Historically, this generalisation is presented as the Rosenbluth scattering formula,

$$\frac{d\sigma}{d\Omega} = \left(\frac{E_3}{E_1}\right)\frac{\alpha^2}{4E_1^2\sin^4\frac{\theta}{2}}\left[\frac{G_E^2(q^2)+\tau G_M^2(q^2)}{1+\tau}\cos^2\frac{\theta}{2} + 2\tau G_M^2\sin^2\frac{\theta}{2}\right] \qquad \text{where } \tau = -\frac{q^2}{4M^2}. \tag{11}$$

where $G_E(q^2)$ and $G_M(q^2)$, known as the electric and magnetic form factors, are a linear combination of $F_1(q^2)$ and $F_2(q^2)$.

$$G_E(q^2) = F_1 + \frac{\kappa_p q^2}{4M^2}F_2 \qquad G_M = \left(F_1+\kappa_p F_2\right) \qquad \text{such that the proton magnetic moment, } \mu_p = \frac{G_M(q^2)}{G_E(q^2)}. \tag{12}$$

These quantities are not derived from first principles but rather measured from data.

Recasting the Rosenbluth equation as a ratio with respect to a simplified Mott scattering expectation (that describes a spinless proton)

$$\left(\frac{d\sigma}{d\Omega}\right)_0 = \left(\frac{E_3}{E_1}\right)\left[\frac{\alpha^2}{4E_1^2\sin^4\frac{\theta}{2}}\cos^2\frac{\theta}{2}\right].$$

$$\frac{d\sigma}{d\Omega}\Big/\left(\frac{d\sigma}{d\Omega}\right)_0 = \frac{G_E^2(q^2)+\tau G_M^2(q^2)}{1+\tau} + 2\tau\ G_M^2(q^2)\ \tan^2\frac{\theta}{2}, \tag{13}$$

Note that this is a linear function of $\tan^2\frac{\theta}{2}$ for fixed τ. The form factors[2] $G_E(q^2)$ and $G_M(q^2)$, are thus deduced.

Phys. Rev. 142(4) (1966) *"Proton Form Factors from Elastic Electron-Proton Scattering"*

In this paper nicely brings together the topics discussed above to measure $G_E(q^2)$ and $G_\mu(q^2)$ from elastic $e^- \to p^+$ Rosenbluth scattering. A beam of [relativistic] electrons, with momentum up to 1000 MeV/c is fired onto a thin liquid hydrogen target. The intensity of the scattered electrons, and their energy, is measured as a function of the scattering angle (θ) by a small spectrometer able to rotate by θ around the hydrogen target.

[1] A neutron has a non-zero $\kappa_n = -1.91$ $\mu_n = \frac{\kappa_n e}{2M_n}$; in the low-energy limit, $F_1(q^2) = 0,\ F_2(q^2) = 1$.

[2] Not the same form factors as in the non-relativistic case. These are dependent on the 4-momentum, q^2 and not the three momentum, $(\underline{q})^2$.

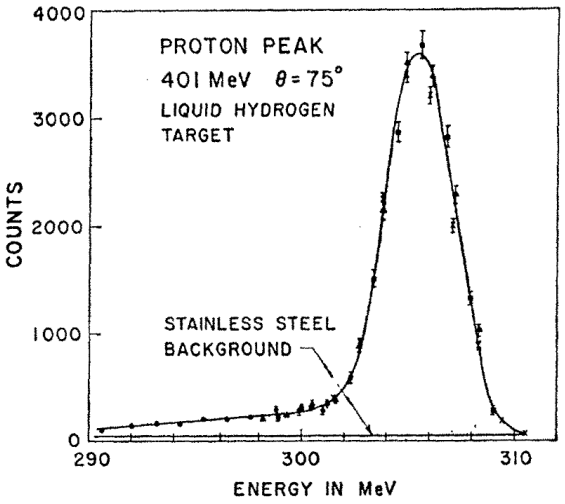
Elastic scattering is ensured selecting only a small range of scattered electron energies, as calculated by Eq. 8,

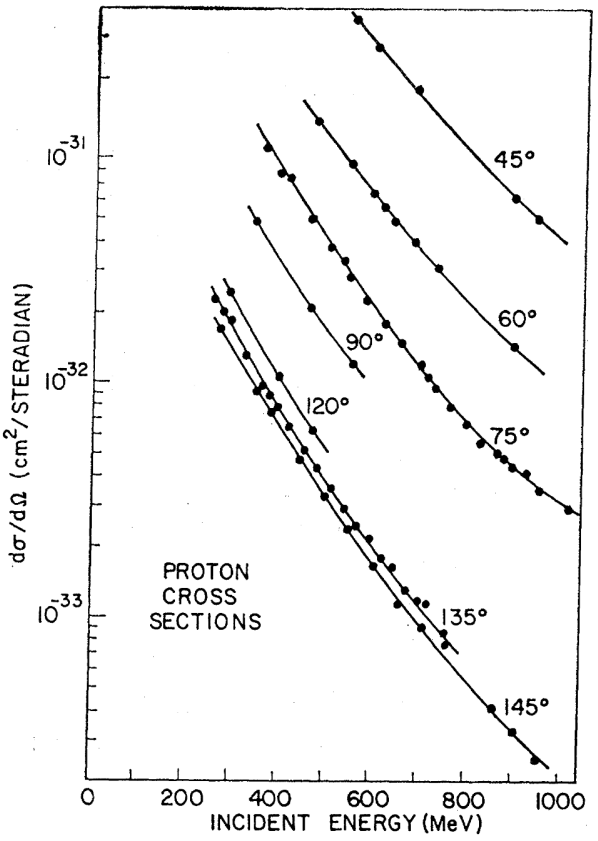
$$E_3 = \frac{E_1 M}{M + E_1(1 - \cos\theta)}$$

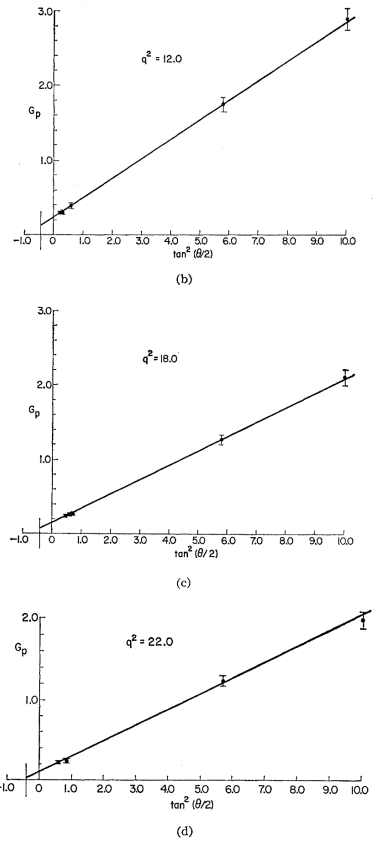
which assumed elastic scattering. In the plot (right) E_1 = 401 MeV and the experiment is rotated to count at 75°.

$$E_3 = \frac{401 \times 938}{938 + 401(1 - \cos 75^\circ)} = 305\,\text{MeV}\,.$$

The data shows the collected data to peak, with little background around this value. Conclusion: the data is *elastic* scatter and Rosenbluth equation is relevant.







The cross section is measured for a variety of angles and incident energies. For each point q^2 is calculated by,

$$q^2 = \frac{ME_1^2(1-\cos\theta)}{M + E_1(1-\cos\theta)}$$

The cross section measurements are used to plot G_P as a function of $\tan^2\frac{\theta}{2}$. The slope and incident, for each fixed value of q^2, is used to calculate the form factors, $G_E(q^2)$ and $G_M^2(q^2)$ as a function of q^2. The plot shows

$$F_{ch} = G_E(q^2) \text{ and } F_{mag} = \frac{G_M(q^2)}{\mu_p}.$$

where the proton magnetic moment,

$$\mu_p = (1+\kappa_p)\mu_{Dirac} = 2.79\mu_{Dirac}.$$

This confirms the proton as an extended object. Also it shows the electric charge and magnetic moment are distributed spatially in the same way.

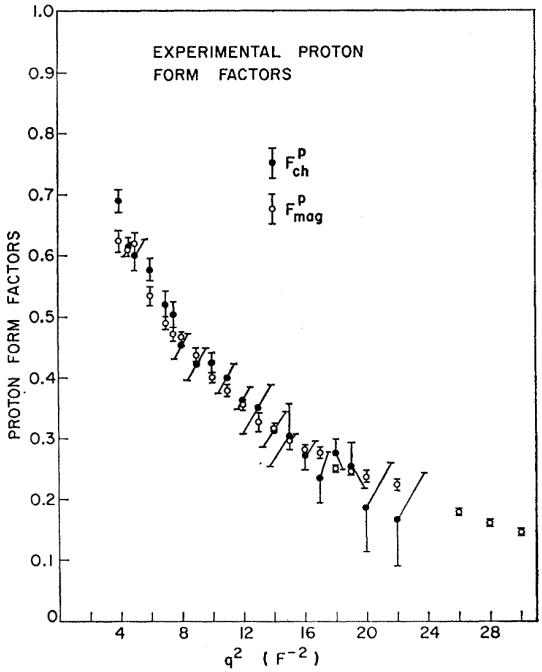


FIG. 5. The experimental values found for the charge and magnetic form factors of the proton as a function of q^2.

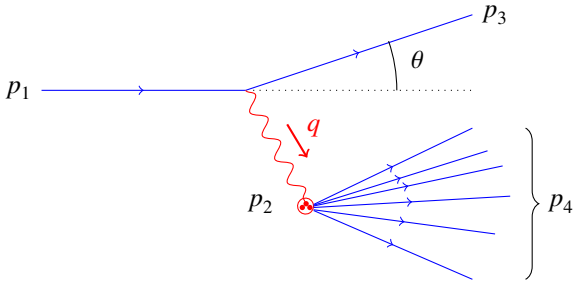
2 Deep inelastic scattering

With sufficiently high-energy electrons ($E_1 > 1\,\text{GeV}$), the proton breaks up forming a shower of hadrons. By baryon-number conservation there at least one baryon in this shower and as the proton is the lowest mass baryon, the invariant mass of this shower must be greater than that of the proton, $p_4^2 > M^2$.

2.1 DIS kinematics

We introduce four useful Lorentz invariant variables,

$$\begin{aligned} Q^2 &= -q^2 \\ x &= \frac{Q^2}{2p_2\cdot q} \\ \nu &= \frac{p_2\cdot q}{M} \\ y &= \frac{p_2\cdot q}{p_2\cdot p_1} \end{aligned}$$



Q^2 can be calculated (as in the elastic case) from the fourmomentum transferred from the electron ($m_e \approx 0$),

$$\begin{aligned} q &= p_1 - p_3 \\ Q^2 = -q^2 &= -(p_1-p_3)^2 \\ &= -\cancel{p_1^2} - \cancel{p_3^2} + 2p_1\cdot p_3 \\ &= 2E_1E_3(1-\cos\theta) \\ &= 4E_1E_3\sin^2\tfrac{\theta}{2} \end{aligned}$$

Let's consider the frame where the target proton is at rest, $p_2 = (M, 0, 0, 0)$,

$$\begin{aligned} p_4^2 = (p_2 + q)^2 &= M^2 - Q^2 + 2p_2 \cdot q \\ \underbrace{p_4^2 - M^2}_{\geq 0} &= 2p_2 \cdot q - Q^2 \\ \quad = \quad 1 \quad &- x \qquad\qquad \therefore \quad \underline{0 < x < 1}\,. \end{aligned}$$

In such a frame, $p_1 = (E_1, 0, 0, E_1)$ and $q = (E_1 - E_3, \underline{p}_1 - \underline{p}_3)$, hence y is the fractional energy loss of the probe,

$$p_1 \cdot p_2 = ME_1 \quad , \quad p_2 \cdot q = M(E_1 - E_3) \qquad \text{so} \qquad y = \frac{p_2 \cdot q}{p_2 \cdot p_1} = \frac{E_1 - E_3}{E_1} \qquad \therefore \quad \underline{0 < y < 1}\,.$$

Similarly, $\nu = (p_2 \cdot q)/M = E_1 - E_3$ is the energy loss, in the frame where the proton target is at rest.

The CoM energy-squared, $s = (p_1 + p_2)^2 = M^2 + 2p_1 \cdot p_2$, neglecting the electron mass. So, $p_1 \cdot p_2 = \frac{1}{2}(s - M^2)$ and,

$$y = \frac{p_2 \cdot q}{p_1 \cdot p_2} = \frac{2M\nu}{s - M^2}\,. \qquad \text{And as} \qquad x = \frac{Q^2}{2M\nu}\,,$$

$$Q^2 = \left(s - M^2\right) xy\,. \tag{14}$$

The s is predefined by the probe and target 4-momenta, M is fixed, so the momentum transfer of the collision is dependent on **two kinematic observables**, $Q^2 = f(x, y)$. Or in terms of the experimental quantities, $Q^2 = f(E_3, \theta)$. This compares with the elastic case (where $x \equiv 1$) which is dependent on just **one kinematic observable**; Eq. 8 is of the form $q^2 = f(\theta)$.

Phys. Lett. B 28(2) (1968) *"Electroproduction of pions near the Δ(1236) isobar and the form factor $G_M^*(q^2)$"*

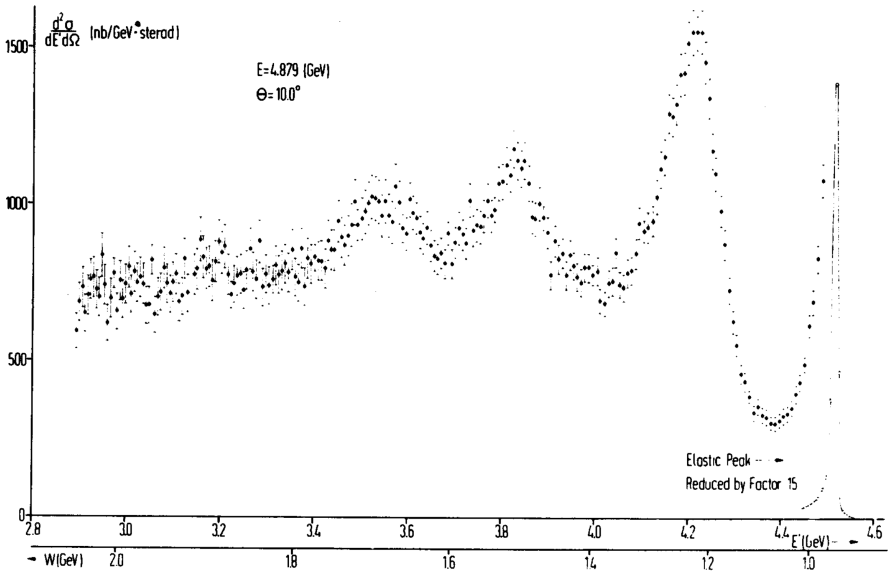


Figure 1: Cross section for electron-proton interaction as a function of scattered probe energy for initial electron energy $E_1 = 4.879$ GeV and scattering angle $\theta = 10^\circ$. The elastic scattering peak is at high $E_3 = 4.522$ GeV at the right of the plot (value calcuable from Eq. 8). Just to the left is the resonance enhancement where $J = I = \frac{3}{2}$ $\Delta(1232)$ baryons are produced. Left of that, as more energy is transferred into the target, the proton breaks up into several particles; this is DIS though some resonance enhancement is still seen.

In this example, the differential cross section for electrons, $p_1 = (E_1, 0, 0, E_1)$ scattering off protons, $p_2 = (M, 0, 0, 0)$ is measured as a function of scattered electron energy and angle. In this setup, $s - M^2 = 2ME_1$, so,

$$Q^2 = 2ME_1xy \qquad = 4E_1E_3\sin^2(\theta/2)\,.$$

Similarly, the invariant mass squared of the proton remnants, p_4^2 (labelled W in the plot below), is fully determined,

$$\begin{aligned} W = p_4^2 &= (p_2 + q)^2 \\ &= M^2 + 2p_2 \cdot q - Q^2 \\ &= M^2 + 2ME_1y - 2ME_1xy \\ &= M^2 + 2ME_1y(1-x) \qquad\qquad \text{in terms of } x, y \end{aligned}$$

or

$$\begin{aligned} &= M^2 + 2M(E_1 - E_3) - 2E_1E_3(1-\cos\theta) \\ &= M^2 + 2ME_1 - 2E_3\left[M + 2E_1\sin^2\tfrac{\theta}{2}\right] \qquad \text{in terms of } \theta, E_3 \end{aligned}$$

For known $E_1 = 4.879$ GeV and specified angle, θ, the scattered electron energy, E_3 gives the remnant mass W is directly.

2.2 Structure functions

With dependence on two kinematic variables necessary, the differential cross section of deep inelastic scattering is written,

$$\frac{d^2\sigma}{dxdQ^2} = \frac{4\pi\alpha^2}{Q^4}\left[\left(1 - y - \frac{M^2x^2y^2}{Q^2}\right)\frac{F_2(x,Q^2)}{x} + y^2\,F_1(x,Q^2)\right]. \tag{15}$$

This is the Lorentz invariant equivalent of the Rosenbluth formula for $p_4^2 > M^2$. In experiments where the proton are initially at rest, we can recast Eq. 15 in terms of the directly measurable quantities, E_3, Ω:

$$\frac{d^2\sigma}{dE_3d\Omega} = \underbrace{\frac{dx}{dE_3}} \cdot \underbrace{\frac{dQ^2}{d\theta}} \cdot \underbrace{\left(\frac{d\Omega}{d\theta}\right)^{-1}} \cdot \frac{d^2\sigma}{dx\,dQ^2}$$

$$\text{as} \quad \overbrace{\frac{2Mx^2}{Q^2}} \quad \overbrace{2E_1E_3\sin\theta} \quad \overbrace{(2\pi\sin\theta)^{-1}}$$

$$\text{from} \quad \overbrace{x = \frac{Q^2}{2M(E_1 - E_3)}} \quad \overbrace{Q^2 = 4E_1E_3\sin^2\tfrac{\theta}{2}} \quad \overbrace{\Omega = 2\pi(1-\cos\theta)}$$

$$\text{so,} \qquad \frac{d^2\sigma}{dE_3d\Omega} = \frac{2Mx^2E_1E_3}{\pi Q^2}\frac{d^2\sigma}{dx\,dQ^2}\,.$$

$$\frac{d^2\sigma}{dE_3d\Omega} = \frac{\alpha^2}{4E_1^2\sin^4\frac{\theta}{2}}\frac{2Mx^2}{(1-y)Q^2}\left[\frac{1}{x}\left(1 - y - \frac{M^2x^2y^2}{Q^2}\right)F_2(x,Q^2) + y^2\,F_1(x,Q^2)\right],$$

as $\frac{E_3}{E_1} = 1 - y$. With careful but trivial manipulation, the following simplifications are achieved,

$$\frac{2Mx^2}{(1-y)Q^2}y^2 = \frac{2}{M}\sin^2\frac{\theta}{2} \qquad\qquad \frac{2Mx}{(1-y)Q^2}\left(1 - y - \frac{M^2x^2y^2}{Q^2}\right) = \frac{1}{E_1 - E_3}\cos^2\frac{\theta}{2}$$

so that,

$$\frac{d^2\sigma}{dE_3d\Omega} = \frac{\alpha^2}{4E_1^2\sin^4\frac{\theta}{2}}\left[\frac{1}{E_1 - E_3}F_2(x,Q^2)\cos^2\frac{\theta}{2} + \frac{2}{M}F_1(x,Q^2)\sin^2\frac{\theta}{2}\right]. \tag{16}$$

An experiment to measure the structure functions can proceed by forming a ratio of cross section with an expectation of such for Mott Scattering for probe energy E_1. Like with the elastic case, this forming a linear relationship with dependent on $\tan^2(\theta/2)$. The structure functions are extracted from the coefficients and the measurement of E_3.

$$\frac{d^2\sigma}{dE_3 d\Omega} \Big/ \left(\frac{d\sigma}{d\Omega}\right)_{\text{Mott}} = \frac{1}{E_1 - E_3} F_2(x, Q^2) + \frac{2}{M} F_1(x, Q^2) \tan^2 \frac{\theta}{2} . \tag{17}$$

Many measurements of cross section and are needed at different scattering angles and E_3 energy bins for the linear relationship to be examined and the structure functions extracted.

2.3 Bjorken scaling and the Callan-Gross relation

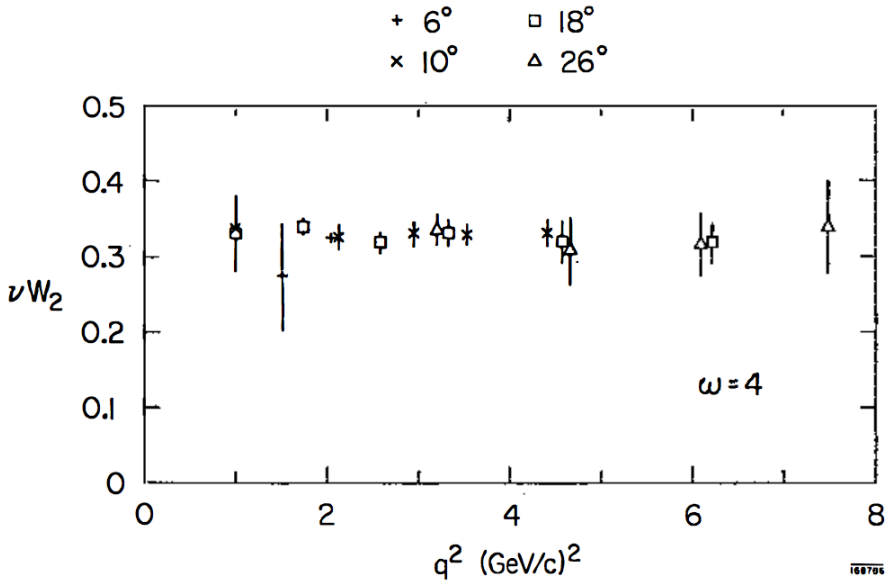


Figure 2: Annu. Rev. Nucl. Sci. 22 (1972) *"Deep inelastic electron scattering"* reviews $F_2(x, Q^2)$ (labelled: νW_2) versus Q^2 (label: q^2) for x = 0.25 (archaic label: $\omega \equiv x^{-1} = 4$). Plot contains measurements from several experiments setup for different scattering angles.

Such measurements of $F_1(x, Q^2)$ and $F_2(x, Q^2)$ are usually shown versus Q^2 in subsets of fixed x as in Fig. 2. The structure functions show a remarkable property: that, for a given x the structure function, and hence scattering cross section, is independent of Q^2. From the definition of x, for constant x, $(E_1 - E_3) \propto Q^2$, meaning that this result says that no matter how much energy is transferred into proton from the electron, the probability to scatter is the same.

This is known as **Bjorken scaling** and was the first evidence that the high-energy electron was scattering off **point-like objects** in the proton.

It is also insightful to alter Eq. 17 to make a comparison with the equivalent ratio from the elastic case,

$$\frac{d^2\sigma}{dE_3 d\Omega}\Bigg/\left(\frac{d\sigma}{d\Omega}\right)_{\text{Mott}} = \frac{F_2(x,Q^2)}{\nu}\left[\ 1\ +\frac{2\nu}{M}\ \frac{F_1(x,Q^2)}{F_2(x,Q^2)}\ \tan^2\frac{\theta}{2}\right],$$

$$\left[\ 1+\frac{2Q^2}{2xM^2}\ \frac{F_1(x,Q^2)}{F_2(x,Q^2)}\tan^2\frac{\theta}{2}\right] \qquad \text{using the definition } x=\frac{Q^2}{2M\nu}\,.$$

$$\left[\ 1\ +\frac{Q^2 x}{\mu^2}\ \frac{F_1(x,Q^2)}{F_2(x,Q^2)}\tan^2\frac{\theta}{2}\right] \qquad \text{introducing a fractional mass, } \mu = xM\,.$$

$$\left[\ 1\ +\ \frac{Q^2}{2\mu^2}\ \tan^2\frac{\theta}{2}\right] \qquad \text{postulating a relationship, } \frac{F_1}{F_2}=\frac{1}{2x}$$

which is the **Callan-Gross relation**. This last formula should be compared with Eq. 9,

$$\frac{d\sigma}{d\Omega}\Bigg/\left(\frac{d\sigma}{d\Omega}\right)_{\text{Mott}} = \left(\frac{E_3}{E_1}\right)\left[\ 1\ -\ \frac{q^2}{2M^2}\ \tan^2\frac{\theta}{2}\right],$$

which described the elastic scattering off the spin-$\frac{1}{2}$, point-particle proton of mass M. In that equation, the second term arises from the "magnetic" spin-spin interaction of electron (spin-$\frac{1}{2}$) and proton (spin-$\frac{1}{2}$). This relation between the two structure functions,

$$\frac{2x\,F_1(x,Q^2)}{F_2(x,Q^2)} = 1\,,$$

bears out in the data and thus strongly indicates the **elastic scattering off point-like, spin-$\frac{1}{2}$ particles of mass $\mu = xM$**. This was the first evidence that quarks are real constituents, rather than *just* a mathematical convenience in describing the symmetries in hadron multiplets.

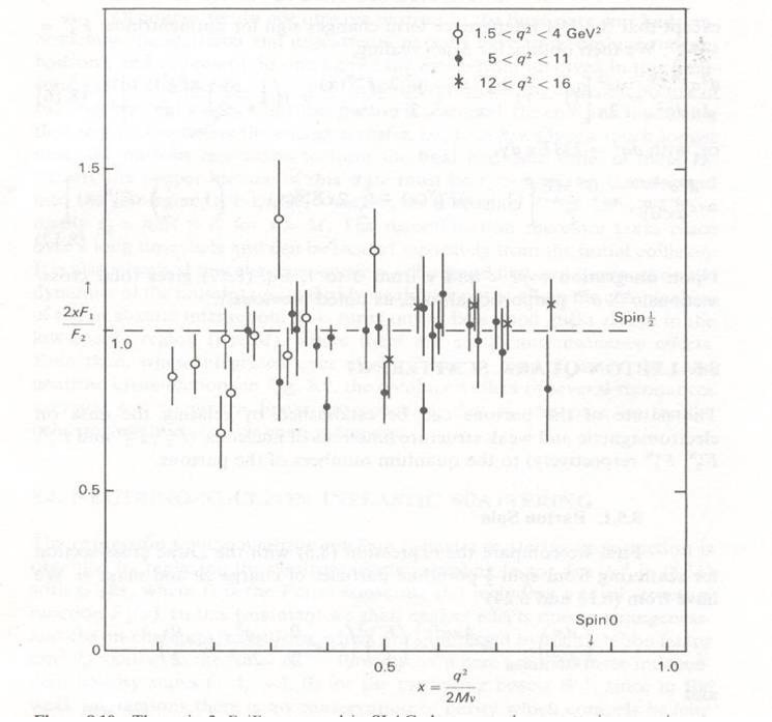


Figure 3: Data supporting the Callan-Gross relation for a large range of x and Q^2.

3 The quark-parton model

This section develops from the concept of scattering off spin-$\frac{1}{2}$ point particles to an understanding of the momentum distributions of the various *parts* of the proton. We consider the centre of mass frame and the "infinite momentum limit" (IML) where $Q^2 \gg M^2$ so mass terms can be neglected.

In the "quark parton model", we imagine the electron is scattered off a quark that is carrying a fraction a of the proton's four-momentum, $p_q = ap_2$, $0 < a < 1$. The scattered quark has four-momentum squared is,

$$\begin{aligned} & (p_q')^2 = (ap_2 + q)^2 \\ \text{so} \quad & (p_q')^2 = a^2 p_2^2 + q^2 + 2ap_2 \cdot q \qquad \text{neglecting masses.} \\ \text{Thus} \quad & a = \frac{Q^2}{2p_2 \cdot q}\,. \end{aligned}$$

This justifies the earlier assertion that Bjorken x is the four-momentum fraction (in the IML).

A quick comparison of the Lorentz Invariant variables for the quark and proton is:

proton :	quark :
$x = \dfrac{Q^2}{2p_2 \cdot q}$	$x_q = 1$ (assume a point particle)
$y = \dfrac{p_2 \cdot q}{p_2 \cdot p_1}$	$y_q = \dfrac{p_2 \cdot q}{p_2 \cdot p_1} = y$
$s = (p_1 + p_2)^2 \approx 2p_1 \cdot p_2$	$s_q = 2xp_1 \cdot p_2 = xs$

3.1 The electron-quark scattering

Consider a high-energy elastic electron-quark collision in the CoM frame. Each fermion has $|\underline{p}^*| = E^* = \sqrt{s_q}/2$.

$p_1 = (E^*, 0, 0, E^*)$ $\quad p_2 = (E^*, 0, 0, -E^*)$ $\quad p_3 = (E^*, E^* \sin\theta^*, 0, E^* \cos\theta^*)$ $\quad p_4 = (E^*, -E^* \sin\theta^*, 0, -E^* \cos\theta^*)$

where θ^* is the CoM scattering angle. From Eq. 5, we take the matrix element for two fermions where the masses are neglected but remembering a quark has fractional charge, e_q,

$$\langle |\mathcal{M}_{fi}|^2 \rangle = 8e_q^2 g_e^4 \frac{(p_1 \cdot p_2)(p_3 \cdot p_4) + (p_1 \cdot p_4)(p_2 \cdot p_3)}{(p_1 - p_3)^4} = 2e_q^2 g_e^4 \frac{4 + (1 + \cos\theta^*)^2}{(1 - \cos\theta^*)^2}\,.$$

The cross section in the CoM frame is taken from the *Basics* lectures, so the $eq \to eq$ differential cross section is,

$$\sigma = \int \frac{|\,\mathcal{M}_{fi}\,|^2}{64\pi^2 s_q} d\Omega^* \qquad \Rightarrow \qquad \frac{d\sigma}{d\Omega^*} = \frac{e_q^2 g_e^4}{32\pi^2 s_q} \frac{4 + (1 + \cos\theta^*)^2}{(1 - \cos\theta^*)^2}\,.$$

Plugging in $g_e = \sqrt{4\pi\alpha}$, this expression is recast in a Lorentz invariant form using,

$$q^2 \approx -2p_1 \cdot p_3 = -2(E^*)^2(1 - \cos\theta^*) = -s_q(1 - \cos\theta^*)/2 \qquad \text{or} \qquad (1 - \cos\theta^*) = -\frac{2q^2}{s_q}\,.$$

$$\begin{aligned} \frac{d\sigma}{dq^2} &= \underbrace{\left(\frac{dq^2}{d\theta^*}\right)^{-1}} \cdot \underbrace{\frac{d\Omega^*}{d\theta^*}} \cdot \underbrace{\frac{d\sigma}{d\Omega^*}} \\ & \qquad \frac{-2}{s_q \sin\theta^*} \quad 2\pi \sin\theta^* \quad \frac{16\pi^2\alpha^2 e_q^2}{32\pi^2 s_q} \quad \frac{4\left(1 + \frac{1}{4}(1 + \cos\theta^*)^2\right)}{4q^4/s_q^2}\,, \end{aligned}$$

$$= -\frac{2\pi\alpha^2 e_q^2}{q^4}\left(1+\tfrac{1}{4}(1+\cos\theta^*)^2\right)$$

Then, $\frac{1}{4}(1+\cos\theta^*)^2 = \frac{1}{4}\left[(1-\cos\theta^*)^2+4\cos\theta^*\right] = \frac{1}{4}\left(\frac{4q^4}{s_q^2}+4+\frac{8q^2}{s_q}\right) = \left(1+\frac{q^2}{s_q}\right)^2$ because, $\cos\theta^* = 1+\frac{2q^2}{s_q}$.

$$\frac{d\sigma}{dq^2} = -\frac{2\pi\alpha^2 e_q^2}{q^4}\left(1+\left(1+\frac{q^2}{s_q}\right)^2\right), \tag{18}$$

The last step is to use the invariant relation, $Q^2 = (s-M^2)xy$, applied to the quark: $M=0$, $x\equiv 1$. Thus, $y = \frac{-q^2}{s_q}$ so,

$$\frac{d\sigma}{dq^2} = -\frac{4\pi\alpha^2 e_q^2}{q^4}\left[1-y+\frac{y^2}{2}\right]. \tag{19}$$

3.2 Relating the QPM to the structure functions

Thinking of the proton again, Eq. 19 is the valid for the differential cross section (vs. $Q^2{=}{-}q^2$) for a quark with given x,

$$\left(\frac{d\sigma}{dQ^2}\right)_x = \frac{4\pi\alpha^2 e_q^2}{Q^4}\left[(1-y)+\frac{y^2}{2}\right].$$

Then we sum over all quarks in the proton with momentum fraction x and integrate over all x,

$$\frac{d\sigma}{dQ^2} = \int_x \left(\frac{d\sigma}{dQ^2}\right)_x q^p(x)\,dx,$$

where we introduce a **parton distribution function $q^p(x)$**, which is the number density of partons of type q in the proton (p) with momentum fraction x. Note that this is a function of x, not Q^2 because the parton density is a property of the proton, not the scattering process. Thus the double-differential cross section for the whole proton, in the quark-parton model becomes,

$$\frac{d^2\sigma}{dx\,dQ^2} = \frac{4\pi\alpha^2}{Q^4}\left[\frac{1}{x}(1-y)+\frac{y^2}{2x}\right] \times\; x\sum_q e_q^2 q^p(x), \tag{20}$$

which we compare to Eq. 15 (the expression with structure functions from deep inelastic scattering) with $M^2y^2 \ll Q^2$:

$$\frac{d^2\sigma}{dxdQ^2} = \frac{4\pi\alpha^2}{Q^4}\left[\frac{1}{x}(1-y)\;F_2(x,Q^2) \;+\; y^2\;F_1(x,Q^2)\right],$$

to arrive at a fundamental definition of the structure functions in the quark-parton model for high energy collisions,

$$2\,x\,F_1(x,Q^2) \xleftrightarrow{\text{Callan-Gross}} F_2(x,Q^2) \xrightarrow{\text{Bjorken scaling}} \qquad F_2(x) = x\sum_q e_q^2\,q^p(x) \tag{21}$$

The quark-parton model of nucleons can thus be tested against experimental measurements of structure functions.

- $e \to p$ scattering:

$$F_2^p(x) = x\left[\frac{4}{9}u^p(x)+\frac{1}{9}d^p(x)\right], \tag{22}$$

  where $u^p(x)$ and $d^p(x)$ are the parton distribution functions for the up and down valence quarks.

- $e \to n$ scattering:

$$F_2^n(x) = x\left[\frac{4}{9}u^n(x) + \frac{1}{9}d^n(x)\right], \tag{23}$$

but if we apply isospin symmetry and say the proton is identical to the neutron except for the $u \leftrightarrow d$ switch, we can say the up quarks will have the same momentum distribution in the proton as down quarks have in the neutron. So,

$$u^n(x) \simeq d^p(x) \qquad \text{and} \qquad d^n(x) \simeq u^p(x)\,.$$

By integrating over x we find $f_{u,d}$, the momentum fractions of the proton (i.e number density times x) carried by up and down quarks.

$$\text{proton:} \quad \int_0^1 F_2^p(x)\,dx = \int_0^1 x\left[\tfrac{4}{9}u^p(x) + \tfrac{1}{9}d^p(x)\right]dx = \frac{4}{9}f_u + \frac{1}{9}f_d\,, \tag{24}$$

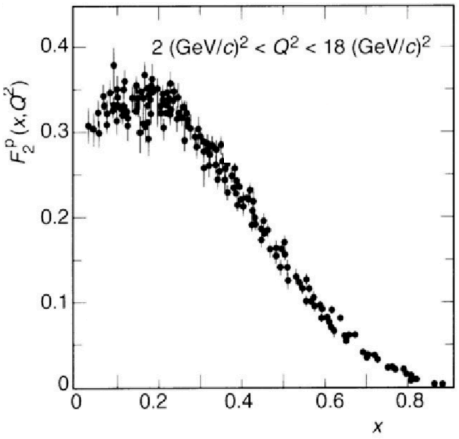
$$\text{neutron:} \quad \int_0^1 F_2^n(x)\,dx = \int_0^1 x\left[\tfrac{4}{9}d^p(x) + \tfrac{1}{9}u^p(x)\right]dx = \frac{1}{9}f_u + \frac{4}{9}f_d\,. \tag{25}$$

To recap: from scattering cross section measurements (vs. scattering angle, θ and scattered electron energy, E_3), the structure function, $F_2(x, Q^2)$ is measured across a wide range of x (x, y, ν, Q^2 calculated from M, E_1, E_3, θ). A plot of $F_2(x, Q^2)$ vs. x is shown on the right. The integral of this distribution is the fraction of proton four-momentum carried by the charged partons (the quarks).

$$\text{proton:} \quad \int_0^1 F_2^p(x)\,dx \approx 0.18$$

From similar measurements with a deuterium target the same estimate is made for the neutron, once the protons contribution to the scattering is subtracted,

$$\text{neutron:} \quad \int_0^1 F_2^n(x)\,dx \approx 0.12\,.$$



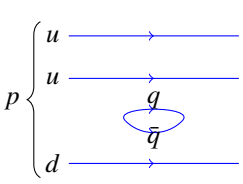
$F_2^p(x, Q^2)$ measurements vs. Bjorken x.

Rearranging these numbers into Eq. 24 and 25 shows only half of the proton's four momentum is carried by the quarks,

$$f_u \approx 0.36 \qquad f_d \approx 0.18 \qquad \Rightarrow \qquad f_u + f_d \approx 0.54\,.$$

3.3 Sea quarks

Quantum fluctuations of the vacuum spontaneously produced $q\bar{q}$ pairs which also interact with the electron and count toward scattering structure. We modify Eq. 22,23 to include $\overline{u}(x)$ and $\overline{d}(x)$,



$$F_2^p(x) = x\left[\tfrac{4}{9}u^p(x) + \tfrac{1}{9}d^p(x) + \tfrac{4}{9}\overline{u}(x) + \tfrac{1}{9}\overline{d}(x)\right] \tag{26}$$

$$F_2^n(x) = x\left[\tfrac{4}{9}d^p(x) + \tfrac{1}{9}u^p(x) + \tfrac{4}{9}\overline{d}(x) + \tfrac{1}{9}\overline{u}(x)\right] \tag{27}$$

for an isoscalar target with equal protons and neutrons, take the average,

$$F_2^N(x) = \tfrac{1}{2}\left(F_2^p(x) + F_2^n(x)\right) = \tfrac{5}{18}x\left[u^p(x) + \overline{u}(x) + d^p(x) + \overline{d}(x)\right] \tag{28}$$

If we label the valance quarks, q_v and require of the sea quarks,

$$u_s(x) \;=\; \overline{u}(x) \;\text{ and }\; d_s(x) \;=\; \overline{d}(x)\,,$$

the parton model becomes,

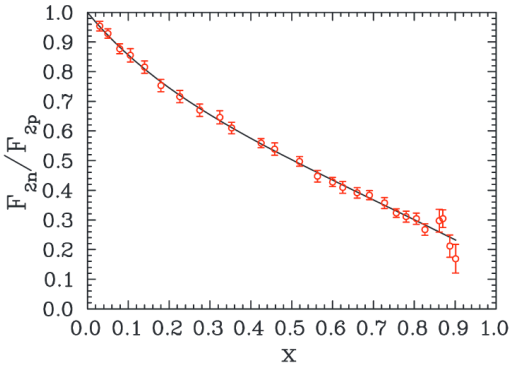
$$F_2^p(x) = x\left[\tfrac{4}{9}u_v^p(x) + \tfrac{1}{9}d_v^p(x) + 2\left(\tfrac{4}{9}\overline{u}(x) + \tfrac{1}{9}\overline{d}(x)\right)\right] \qquad (29)$$

$$F_2^n(x) = x\left[\tfrac{4}{9}d_v^p(x) + \tfrac{1}{9}u_v^p(x) + 2\left(\tfrac{4}{9}\overline{d}(x) + \tfrac{1}{9}\overline{u}(x)\right)\right] \qquad (30)$$

The data, shows (right), shows

$$F_2^n(x) \,/\, F_2^p(x) \to 1 \quad \text{as} \quad x \to 0\,,$$

which shows a dominance of sea quark interactions at low-x.



J. Phys. G: Nucl. Part. Phys. **36** (2009) 025005.

At $x \approx \frac{1}{3}$ (more like 0.28) the ratio of structure functions is about 0.66 in the data. This matches with the naïve expectation where $\overline{u}(x), \overline{d}(x)$ are neglected and there are 2:1 $u : d$ valance quarks, all sharing one-third of the proton fourmomentum.

$$\frac{F_2^n(x)}{F_2^p(x)} = \frac{\frac{4}{9}\,\cancel{d_v^p(x)}^{\,1} + \frac{1}{9}\,\cancel{u_v^p(x)}^{\,2}}{\frac{4}{9}\,\cancel{u_v^p(x)}^{\,2} + \frac{1}{9}\,\cancel{d_v^p(x)}^{\,1}} = \frac{4+2}{8+1} = 0.66 \quad \text{(naïve assumption : } x \equiv \tfrac{1}{3},\; u^p = 2,\; d^p = 1)\,.$$

At even higher x, the structure function ratio decreases further. This implies that the more-numerous quark (u in the proton, d in the neutron) has a harder momentum spectrum than the quark of opposite isospin.

3.4 Gottfried Sum Rule

The Gottfried Sum Rule tests the difference in the proton and neutron PDFs. It quantifies a flavour asymmetry assuming an equal number of q and $\overline{q}$ in pair-production,

$$\begin{aligned} S_G = \int_0^1 \frac{F_2^p(x) - F_2^n(x)}{x}dx = & \int_0^1 \left[\frac{4}{9}u_v^p(x) + \frac{1}{9}d_v^p(x) + 2\left(\frac{4}{9}\overline{u}(x) + \frac{1}{9}\overline{d}(x)\right)\right] \\ & - \left[\frac{1}{9}u_v^p(x) + \frac{4}{9}d_v^p(x) + 2\left(\frac{4}{9}\overline{d}(x) + \frac{1}{9}\overline{u}(x)\right)\right] dx \\ = \frac{1}{9}\int_0^1 3u_v^p(x)\,dx + & \frac{1}{9}\int_0^1 -3d_v^p(x)\,dx + \frac{2}{9}\int_0^1 \left[3\overline{u}(x) - 3\overline{d}(x)\right]\,dx \end{aligned}$$

$$S_G = \frac{1}{3} + \frac{2}{3}\int_0^1 \left[\overline{u}(x) - \overline{d}(x)\right]\,dx\,.$$

The one-third term appears because integrated over all momentum fraction, there are two u valance quarks and one valance d quark in the proton.

With equal number of $\overline{u}$ and $\overline{d}$ in the Sea, The Gottfried Sum should be measured close to 0.333. The NMC experiment measures, in the range $0.004 < x < 0.8$,

$$S_G = 0.228 \pm 0.007\,.$$

This is significantly less than 0.333 demonstrating there are more $d\overline{d}$ pairs produced inside the proton quantum sea than $u\overline{u}$ pairs.

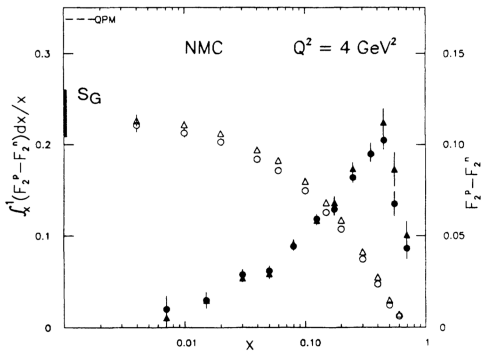


FIG. 1. The difference $F_2^p - F_2^n$ (full symbols and scale to the right) and $\int_x^1 (F_2^p - F_2^n)dx/x$ (open symbols and scale to the left) at $Q^2 = 4$ GeV^2, as a function of x from the present reevaluation (circles) and from Ref. [1] (triangles). The extrapolated result S_G from the present work and the prediction of the simple quark-parton model (QPM) are also shown.

4 DIS with neutrino probes

Measuring scattering cross sections with neutrino and antineutrino probes is a powerful extension to the charged-lepton DIS experiments considered earlier. Assuming the relativistic case ($E >> m_p$), the quark's helicity eigenstate aligns with its inherent chirality. Then using the maximally parity-violating properties neutrinos, the quark and antiquark content of the nuclear matter is distinguished.

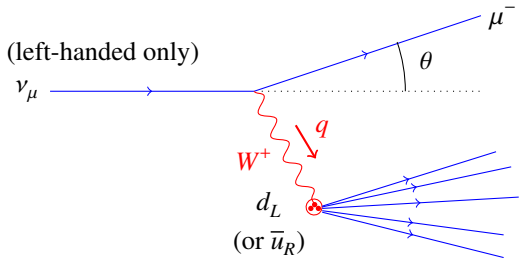
We imagine a neutrino with energy $20 - 40$ GeV such that $|q| << m_W$ so the propagator term for the weak force,

$$\text{propagator} \simeq \frac{ig_{\mu\nu}}{m_W^2},$$

independent of $|q|$. The vertex factor becomes,

$$i\gamma^\mu \frac{g_W}{\sqrt{2}} \tfrac{1}{2}(1-\gamma^5),$$

which couples to left-hand quarks and right-handed anti-quarks.



4.1 neutrino-quark scattering

Similarly to Eq. 3 (electromagnetic interaction), the matrix element for this weak interaction is,

$$-i\mathcal{M}_{fi} = \left[\bar{u}(p_3)\frac{ig_w}{\sqrt{2}}\gamma^\mu \tfrac{1}{2}(1-\gamma^5)u(p_1)\right]\frac{ig_{\mu\nu}}{m_W^2}\left[\bar{u}(p_4)\frac{ig_w}{\sqrt{2}}\gamma^\nu \tfrac{1}{2}(1-\gamma^5)u(p_2)\right] \tag{31}$$

$$\mathcal{M}_{fi} = \frac{g_w^2}{2m_W^2}\left[\bar{u}_L(p_3)\gamma^\mu u_L(p_1)\right]\left[\bar{u}_L(p_4)\gamma_\mu u_L(p_2)\right] \tag{32}$$

$$= \frac{g_w^2}{2m_W^2}\left[\bar{u}_\downarrow(p_3)\gamma^\mu u_\downarrow(p_1)\right]\left[\bar{u}_\downarrow(p_4)\gamma_\mu u_\downarrow(p_2)\right], \tag{33}$$

as chirality is equivalent to helicity in the limit. We don't use the spin-averaged result anymore because the neutrino picks out one chiral state. Use the **negative** helicity state, $u_\downarrow$.

$$u_\downarrow = \sqrt{E+m}\begin{pmatrix} -\sin\frac{\theta}{2} \\ e^{i\phi}\cos\frac{\theta}{2} \\ \frac{|\mathbf{p}|}{E+m}\sin\frac{\theta}{2} \\ \frac{-|\mathbf{p}|}{E+m}e^{i\phi}\cos\frac{\theta}{2} \end{pmatrix},$$

where the coordinate system is set up such that $\mathbf{p}_1$ is along the z-axis ($\theta = 0$) and the scattered lepton lies in the $\phi = 0$ plane and the scattered quark has $(\theta, \phi) = (180^\circ - \theta^*, 180^\circ)$. Thus in the CoM relativistic limit where $m = 0$, $E = |\mathbf{p}|$,

$$u_\downarrow(p_1) = \sqrt{E}\begin{pmatrix} 0 \\ 1 \\ 0 \\ -1 \end{pmatrix}, \qquad u_\downarrow(p_2) = \sqrt{E}\begin{pmatrix} -1 \\ 0 \\ 1 \\ 0 \end{pmatrix}, \qquad u_\downarrow(p_3) = \sqrt{E}\begin{pmatrix} -\sin\frac{\theta^*}{2} \\ \cos\frac{\theta^*}{2} \\ \sin\frac{\theta^*}{2} \\ -\cos\frac{\theta^*}{2} \end{pmatrix}, \qquad u_\downarrow(p_4) = \sqrt{E}\begin{pmatrix} -\cos\frac{\theta^*}{2} \\ -\sin\frac{\theta^*}{2} \\ \cos\frac{\theta^*}{2} \\ \sin\frac{\theta^*}{2} \end{pmatrix}.$$

The calculation of Eq. 33 has two parts, the first of which is,

$$\bar{u}_\downarrow(p_3)\gamma^\mu u_\downarrow(p_1)$$
$$= u_\downarrow^*(p_3)\gamma^0\gamma^\mu u_\downarrow(p_1)$$

The $\gamma^0\gamma^\mu$ must be calculated from the standard definition of the gamma matrices (Dirac rep^n),

$$\gamma^0\gamma^0 = \begin{pmatrix} 1 & & & \\ & 1 & & \\ & & 1 & \\ & & & 1 \end{pmatrix} \qquad \gamma^0\gamma^1 = \begin{pmatrix} & & & 1 \\ & & 1 & \\ & 1 & & \\ 1 & & & \end{pmatrix} \qquad \gamma^0\gamma^2 = \begin{pmatrix} & & & -i \\ & & i & \\ & -i & & \\ i & & & \end{pmatrix} \qquad \gamma^0\gamma^3 = \begin{pmatrix} & & 1 & \\ & & & -1 \\ 1 & & & \\ & -1 & & \end{pmatrix}$$

Multiplying through, we get,

$$\bar{u}_\downarrow(p_3)\,\gamma^\mu\,u_\downarrow(p_1) = 2E\begin{pmatrix} \cos\frac{\theta^*}{2} \\ \sin\frac{\theta^*}{2} \\ -i\sin\frac{\theta^*}{2} \\ \cos\frac{\theta^*}{2} \end{pmatrix}.$$

Similarly for the second part of the matrix element calculation,

$$\bar{u}_\downarrow(p_4)\,\gamma^\nu\,u_\downarrow(p_2) = 2E\begin{pmatrix} \cos\frac{\theta^*}{2} \\ -\sin\frac{\theta^*}{2} \\ -i\sin\frac{\theta^*}{2} \\ -\cos\frac{\theta^*}{2} \end{pmatrix}$$

So that all together with $g_{\mu\nu} = (1,-1,-1,-1)$,

$$\begin{aligned} \left[\bar{u}_\downarrow(p_3)\,\gamma^\mu\,u_\downarrow(p_1)\right] g_{\mu\nu} \left[\bar{u}_\downarrow(p_4)\,\gamma^\nu\,u_\downarrow(p_2)\right] &= 4E^2\left(\cos^2\tfrac{\theta^*}{2} + \sin^2\tfrac{\theta^*}{2} + \sin^2\tfrac{\theta^*}{2} + \cos^2\tfrac{\theta^*}{2}\right) \\ &= 8E^2 \\ \text{So,} \quad \mathcal{M}_{fi} &= \frac{g_w^2}{2m_w^2}8E^2 = \frac{g_w^2}{m_w^2}\hat{s} \end{aligned}$$

as $\hat{s} = (2E)^2$ is the CoM energy of the neutrino-quark system, as distinct from the neutrino-proton CoM energy, $\sqrt{s}$,

$$\begin{aligned} p_\nu^* &= \tfrac{\sqrt{s}}{2}(1,0,0,1) \quad p_q^* = \tfrac{x\sqrt{s}}{2}(1,0,0,-1) \\ \sqrt{\hat{s}} &= p_\nu^* + p_q^* = \tfrac{\sqrt{s}}{2}((1+x),0,0,(1-x)) \\ \hat{s} &= \tfrac{s}{4}((1+x)^2 - (1-x)^2) \\ &= sx \end{aligned}$$

NB: The same quantity for e^+e^- scattering was $\mathcal{M}_{fi} = \frac{g_e^2}{q^2}\hat{s}(1+\cos\theta) = g_e^2(1+\cos\theta)$. By neglecting the q^2 term in the denominator of the weak propagator, a dependence on the CoM energy, $\hat{s}$ remains in the matrix element.

We continue in the CoM frame. From *Relativistic Kinematics*, the differential cross section is,

$$\frac{d\sigma}{d\Omega} = \frac{1}{64\pi^2\hat{s}}\frac{|p_f^*|}{|p_i^*|}\left|\mathcal{M}_{fi}\right|^2 \cdot \frac{1}{2}$$

as the quark will be in a spin-aligned helicity state half the time and will not participate in the weak interaction. Averaging over all spins this introduces the extra factor $\frac{1}{2}$. So with a reminder of the natural units conversion,

$$\frac{d\sigma}{d\Omega^*} = \frac{g_w^4}{128\pi^2 m_w^4}\hat{s} \quad = \frac{G_F^2}{4\pi^2}\hat{s} \quad \text{where } G_F/(\hbar c)^3 = \frac{\sqrt{2}g_w^2}{8m_w^2} = 1.16\times10^{-5}\,\text{GeV}^{-2}\,.$$

And observing that there is no angular dependence in this differential cross section and $\int d\Omega^* = 4\pi$,

$$\sigma_{\nu q} = \frac{G_F^2}{\pi}\hat{s}\,(\hbar c)^2\,.$$

4.2 neutrino-antiquark scattering

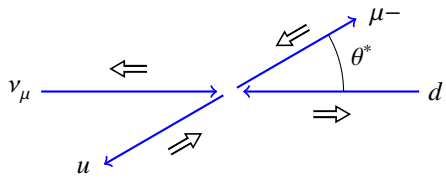
We proceed in a similar manner but the quark current is travelling backwards in time,

$$-i\mathcal{M}_{fi} = \left[\bar{u}(p_3)\,\frac{ig_w}{\sqrt{2}}\gamma^\mu\tfrac{1}{2}(1-\gamma^5)\,u(p_1)\right]\,\frac{ig_{\mu\nu}}{m_W^2}\,\left[\bar{v}(p_2)\,\frac{ig_w}{\sqrt{2}}\gamma^\nu\tfrac{1}{2}(1-\gamma^5)\,v(p_4)\right]$$

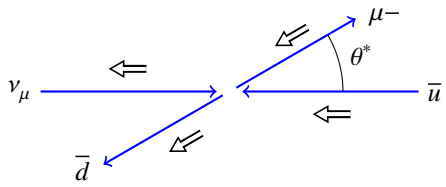
$$\mathcal{M}_{fi} = \frac{g_w^2}{2m_W^2}\left[\bar{u}_L(p_3)\,\gamma^\mu\,u_L(p_1)\right]\left[\bar{v}_R(p_2)\,\gamma_\mu\,v_R(p_4)\right]$$

$$\mathcal{M}_{fi} = \frac{g_w^2}{2m_W^2}\left[\bar{u}_\downarrow(p_3)\,\gamma^\mu\,u_\downarrow(p_1)\right]\left[\bar{v}_\uparrow(p_2)\,\gamma_\mu\,v_\uparrow(p_4)\right]$$

which looks very similar to matrix element for neutrino-quark scattering except that there is a subtle angular momentum dependence. In νq scattering the total angular momentum of the initial state is $J = 0$, but in the $\nu\bar{q}$ case the spins are aligned, $J = 1$ and the transition will depend on a rotation matrix element to conserve angular momentum.



νq scattering. $J = 0:\ \mathcal{M}_{fi} \propto d^0_{0,0}$



$\nu\bar{q}$ scattering. $J = 1:\ \mathcal{M}_{fi} \propto d^1_{-1,-1}$

Inserting the rotation $d^1_{-1,-1}$,

$$\mathcal{M}_{\nu\bar{q}} = \mathcal{M}_{\nu q}\cdot\tfrac{1}{2}(1+\cos\theta^*) \qquad \Rightarrow \qquad \frac{d\sigma_{\nu\bar{q}}}{d\Omega^*} = \frac{d\sigma_{\nu q}}{d\Omega^*}\cdot\frac{1}{4}(1+\cos\theta^*)^2$$

and integrating over solid angle,

$$\sigma_{\nu\bar{q}} = \int_0^{2\pi}\int_{+1}^{-1}\frac{G_F^2}{4\pi^2}\hat{s}\cdot\frac{1}{4}(1+\cos\theta^*)^2 d(\cos\theta^*) \tag{34}$$

$$= \frac{G_F^2}{8\pi}\hat{s}\left[\frac{1}{3}(1+\cos\theta^*)^3\right]_{-1}^{+1} \tag{35}$$

$$= \frac{G_F^2}{3\pi}\hat{s}. \tag{36}$$

The antineutrino-antiquark and antineutrino-quark scattering cross sections are identical to that of their *CP* conjugate processes,

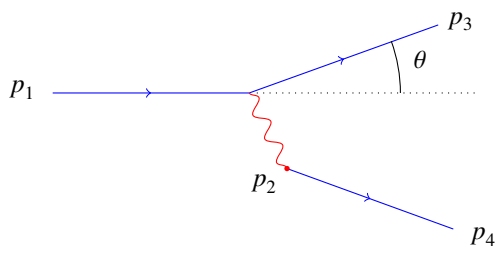
$$\sigma_{\bar{\nu}\bar{q}} = \sigma_{\nu q} = \frac{G_F^2}{\pi}\hat{s} \qquad\qquad \sigma_{\bar{\nu}q} = \sigma_{\nu\bar{q}} = \frac{G_F^2}{3\pi}\hat{s}\,.$$

From these results we could be tempted to make a preliminary (and wrong) conclusion that the cross section for antineutrino scattering off a matter target will be one third that in neutrino scattering.

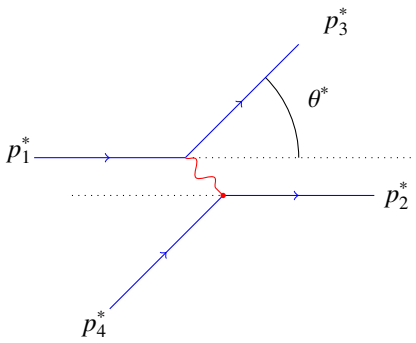
4.3 Lorentz invariant differential cross section

In the same manner as done with electron probes, let's switch to a Lorentz-invariant form as this allows for an easier conversion from the laboratory frame in which an experimental measurement is made. Let's consider the lab and CoM cases in parallel and calculate the Lorentz-invariant variable, y.

Lab.



CoM



$$p_1 = (E_\nu, 0, 0, E_\nu)$$
$$p_2 = (m_q, 0, 0, 0)$$
$$p_3 = (E_\mu, E_\mu \sin\theta, 0, E_\mu \cos\theta)$$
$$p_1 - p_3 = q = \begin{pmatrix} E_\nu - E_\mu \\ -E_\mu \sin\theta \\ 0 \\ E_\nu - E_\mu \cos\theta \end{pmatrix}$$
$$y = \frac{q \cdot p_2}{p_1 \cdot p_2} = \frac{m_q(E_\nu - E_\mu)}{m_q E_\nu} = 1 - \frac{E_\mu}{E_\nu}$$

$$p_1^* = (E^*, 0, 0, E^*)$$
$$p_2^* = (E^*, 0, 0, -E^*)$$
$$p_3^* = (E^*, E^* \sin\theta^*, 0, E^* \cos\theta^*)$$
$$p_1^* - p_3^* = q = \begin{pmatrix} 0 \\ -E^* \sin\theta^* \\ 0 \\ -E^*(1 - \cos\theta^*) \end{pmatrix}$$
$$y = \frac{q \cdot p_2}{p_1 \cdot p_2} = \frac{(E^*)^2(1 - \cos\theta^*)}{2(E^*)^2} = \frac{1}{2}(1 - \cos\theta^*)$$

As before, use chain rule to change variables,

$$\frac{d\sigma_{\nu q}}{dy} = \underbrace{\left|\frac{dy}{d\theta^*}\right|^{-1}}_{\left|\frac{1}{2}\sin\theta^*\right|^{-1}} \underbrace{\frac{d\Omega}{d\theta^*}}_{2\pi\sin\theta^*} \underbrace{\frac{d\sigma}{d\Omega}}_{\frac{G_F^2}{4\pi^2}\hat{s}}$$
$$\frac{d\sigma_{\nu q}}{dy} = \frac{G_F^2 \hat{s}}{\pi}$$

For the neutrino-antiquark scattering, the angular dependence of the rotation matrix element must be transferred to the Lorentz-invariant form,

$$d^1_{-1,-1} = \tfrac{1}{2}(1 + \cos\theta^*) = 1 - \tfrac{1}{2}(1 - \cos\theta^*) = 1 - y$$
$$\text{so,} \quad \frac{d\sigma_{\nu\bar{q}}}{dy} = \frac{G_F^2 \hat{s}}{\pi}(1 - y)^2$$

4.4 Quark-Parton model with neutrino scattering

The next step is to take the differential cross section formulae of the quark and antiquark scattering and apply them to the distribution of the quarks and antiquarks in the nucleons. As before the **number density** of of down quarks in a proton (p) with momentum fraction x is $d^p(x)$. Similarly, the number of anti-up quarks with x in the proton is $\overline{u}^p(x)$. Thus,

$$\begin{aligned}\frac{d\sigma_{\nu p}}{dxdy} &= d^p(x) \cdot \frac{G_F^2}{\pi}\hat{s} \;+\; \overline{u}(x) \cdot \frac{G_F^2}{\pi}\hat{s}(1-y)^2 \\ &= \frac{G_F^2}{\pi}xs\left[d^p(x) + (1-y)^2\overline{u}(x)\right]\end{aligned}$$

where we replace $\hat{s}$ with xs. The cross section for neutrino interactions is so tiny that experiments must use large stationary masses to provoke a sufficient number of weak interactions. Such large targets are approximately isoscalar (e.g. ^{54}Fe, $Z = 26$, $N = 28$) so we also consider the neutron cross section but use an assumption of isospin symmetry of the valance quarks to write the neutron's valance quark **number densities** in terms of that of the proton,

$$\begin{aligned}\frac{d\sigma_{\nu n}}{dxdy} &= \frac{G_F^2}{\pi}xs\underbrace{\left[d^n(x) + (1-y)^2\overline{u}(x)\right]}_{\substack{d^n(x)=u^p(x)\\ \overline{u}(x)=\overline{d}(x)}} \\ &= \frac{G_F^2}{\pi}xs\overbrace{\left[u^p(x) + (1-y)^2\overline{d}(x)\right]}\end{aligned}$$

For a completely isoscalar target the average cross section is,

$$\begin{aligned}\frac{d\sigma_{\nu N}}{dxdy} &= \frac{1}{2}\left[\frac{d\sigma_{\nu p}}{dxdy} + \frac{d\sigma_{\nu n}}{dxdy}\right] \\ &= \frac{G_F^2}{2\pi}xs\left[u^p(x) + d^p(x) + (1-y)^2\left(\overline{u}(x) + \overline{d}(x)\right)\right]\end{aligned}$$

Remembering the structure functions of charged-lepton scattering, Eq. 28, a neutrino scattering analogue is defined:

$$F_2^{\nu N}(x) = x\left[u(x) + d(x) + \overline{u}(x) + \overline{d}(x)\right] \tag{37}$$

Here, the charge is not fractional and the neutrino scattering structure is larger,

$$F_2^N(x) \;=\; \tfrac{5}{18}F_2^{\nu N}(x)\,. \tag{38}$$

A related structure function, $F_3^{\nu N}(x)$ is also defined,

$$F_3^{\nu N}(x) \;=\; u(x) + d(x) - \overline{u}(x) - \overline{d}(x) \tag{39}$$

such that

$$\frac{d\sigma_{\nu N}}{dxdy} = \frac{G_F^2}{2\pi}s\left[\frac{F_2^{\nu N} + xF_3^{\nu N}}{2} + \frac{F_2^{\nu N} - xF_3^{\nu N}}{2}(1-y)^2\right] \tag{40}$$

$$\frac{d\sigma_{\overline{\nu}N}}{dxdy} = \frac{G_F^2}{2\pi}s\left[\frac{F_2^{\nu N} - xF_3^{\nu N}}{2} + \frac{F_2^{\nu N} + xF_3^{\nu N}}{2}(1-y)^2\right] \tag{41}$$

Integrating over all x, we define the momentum fractions (i.e number density times x) of quarks and antiquarks,

$$f_q = \int_0^1 x\left[u^p(x) + d^p(x)\right]dx \;=\; \int_0^1 \frac{F_2^{\nu N} + xF_3^{\nu N}}{2}dx \tag{42}$$

$$f_{\overline{q}} = \int_0^1 x\left[\overline{u}^p(x) + \overline{d}^p(x)\right]dx \;=\; \int_0^1 \frac{F_2^{\nu N} - xF_3^{\nu N}}{2}dx \tag{43}$$

such that the differential cross section with respect to y only becomes,

$$\frac{d\sigma_{\nu N}}{dy} = \frac{G_F^2}{2\pi} s \left[f_q + (1-y)^2 f_{\bar{q}} \right] \tag{44}$$

$$\frac{d\sigma_{\bar{\nu} N}}{dy} = \frac{G_F^2}{2\pi} s \left[(1-y)^2 f_q + f_{\bar{q}} \right] . \tag{45}$$

Gross Llewellyn Smith sum rule

The GLS sum rule notices that $F_3^{\nu N}(x)$ 'counts' the number of valance quarks, $q_{\mathrm{v}}(x) = q^p(x) - \overline{q}^p(x)$.

$$\int_0^1 x F_3^{\nu N}(x) \frac{dx}{x} = \int_0^1 \left[u_{\mathrm{v}}(x) + d_{\mathrm{v}}(x) \right] dx = 3 \tag{46}$$

Measurements conclude $S_{\mathrm{GLS}} = 2.5 \pm 0.2$.

4.5 Neutrino DIS experiments

In the late 1970s a couple of experiments were built to study the kinematics and cross sections of muon neutrinos interacting with matter. Due to their extremely small cross sections, a high intensity (anti)neutrino beam was constructed and large detectors built in a fixed target configuration with respect to the incoming (anti)neutrino beam. The CDHS (Fig. 4) and CHARM experiments occupied the same hall at CERN and shared the conceptual design to measure four momentum of the scattered lepton, p_3, the recoiling hadronic shower (p_4) for a somewhat-defined incoming muon-neutrino beam p_1 on the stationary target, p_2. From the four vectors, the Lorentz invariants, x, y, s, Q^2 are calculated for each event.

Figure 4: CDHS experiment at CERN (1976-1984). The experiment provided electronic readout of both a sampling calorimeter (interleaved iron plates and scintillator) and and a downstream tracking chamber in a magnetic field. Together both the energy of the hadronic shower and the energy and the muon were measured.

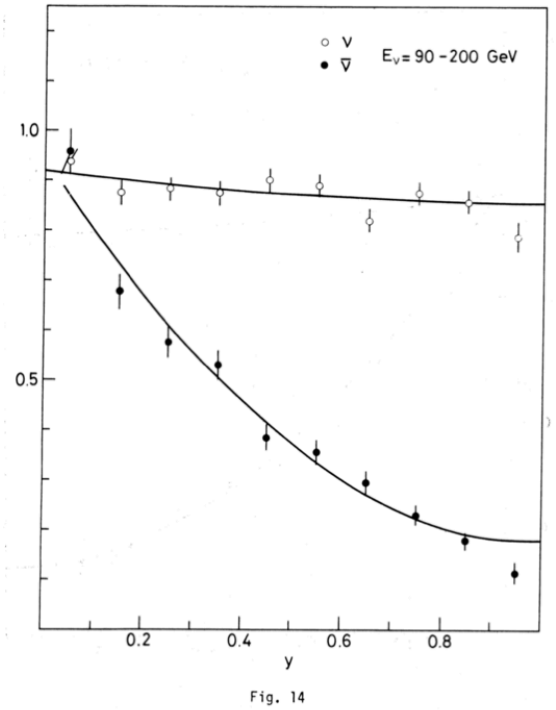


Fig. 14

As above, y is simply calculated from the measured muon energy and the neutrino beam energy,

$$y = 1 - \frac{E_\mu}{E_\nu} \quad \text{where} \quad E_\nu = E_\mu + E_X$$

The CoM energy squared,

$$s = \left(\begin{pmatrix} E_\nu \\ 0 \\ 0 \\ E_\nu \end{pmatrix} + \begin{pmatrix} M_p \\ 0 \\ 0 \\ 0 \end{pmatrix} \right)^2 = 2E_\nu M_p + M_p^2 \approx 2E_\nu M_p \,.$$

so the measured cross section can be applied to the four-momentum fraction equations, Eq. 43 and Eq. 45.
Such (anti)neutrino scattering data is shown on the left. The ν curve shows a small angular dependance which originates from the the antiquark scattering. The antineutrino curve drops dramatically as the quark scattering, which has the angular dependant $(1-y)^2$ term, dominates.

The final step is to integrate over y,

$$\int_0^1 (1-y)^2 dy = \left[-\frac{1}{3}(1-y)^3 \right]_0^1 = \frac{1}{3} \,,$$

so the total cross sections for (anti)neutrino scattering are,

$$\sigma_{\nu N} = \frac{G_F^2}{2\pi} s \left[f_q + \frac{1}{3} f_{\bar{q}} \right] \qquad \sigma_{\bar{\nu} N} = \frac{G_F^2}{2\pi} s \left[f_{\bar{q}} + \frac{1}{3} f_q \right] .$$

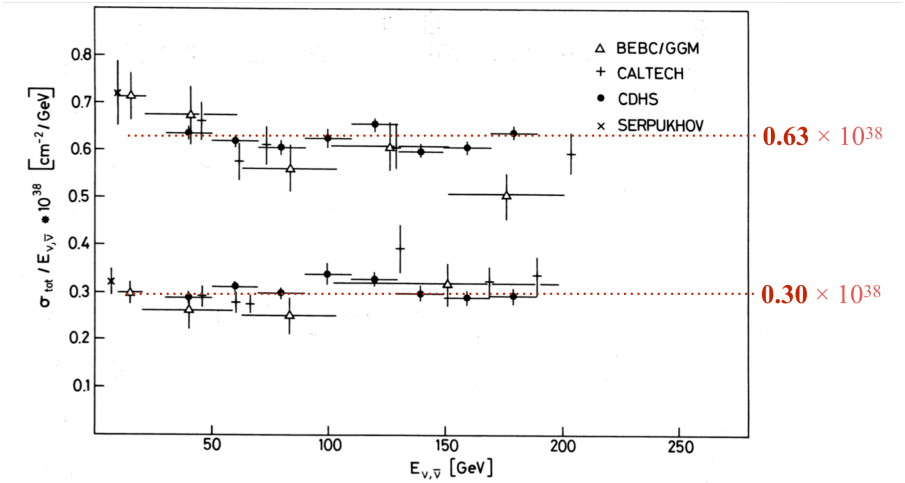


Figure 5: Total (anti)neutrino cross section vs. the neutral lepton's beam energy. Data taken from several neutrino scattering experiments, the most precise of which is CHGS, discussed in the text. Note the Bjorken scaling and the relative size of $\sigma_{\nu_\mu N}$ and $\sigma_{\bar{\nu}_\mu N}$: ~ 2.

Data showing the total (anti)neutrino cross section versus probe lepton energy is show in Fig. 5. Once again the Bjorken scaling seems to hold well. The second feature is the relative magnitude of total cross sections,

$$\nu_e \text{ scattering cross section: } \propto \quad f_q + \frac{1}{3} f_{\bar{q}} \approx 0.63 \tag{47}$$

$$\bar{\nu}_e \text{ scattering cross section: } \propto \quad f_{\bar{q}} + \frac{1}{3} f_q \approx 0.30 \tag{48}$$

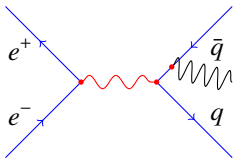
which is close to a factor 2, smaller than the factor 3 predicted for valance quarks only. Taking the ratio of Eqs. 47&48 and rearranging gives,

$$\frac{f_{\bar{q}}}{f_q} = \frac{1}{5}$$

And given electromagnetic data showed $f_q + f_{\bar{q}} = 0.54$, we calculate that f_q is 0.45 and $f_{\bar{q}}$ is just 0.09. Leaving 40-50% of the proton's fourmomentum to be carried by something that couples neither to the electromagnetic nor the weak forces: gluons.

5 The gluon

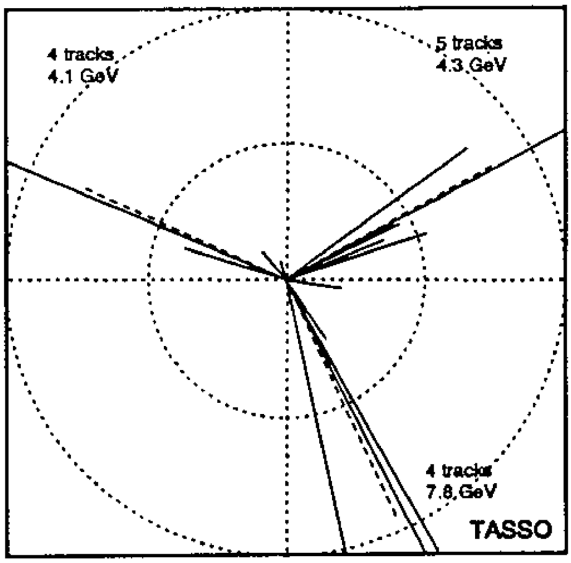
In the 1970s, QCD was a considered only a candidate theory of the of the strong force but its prediction of the force-carrying spin-1 particle was unique. A series of experiments examined the production of hadronic jets from high-energy e^+e^- collisions ($\sqrt{s} \approx 20$ GeV) in particular to look for rare three jet events corresponding to the diagram,



Moreover the rate of such should depend on the strong coupling constant. The experiments found,

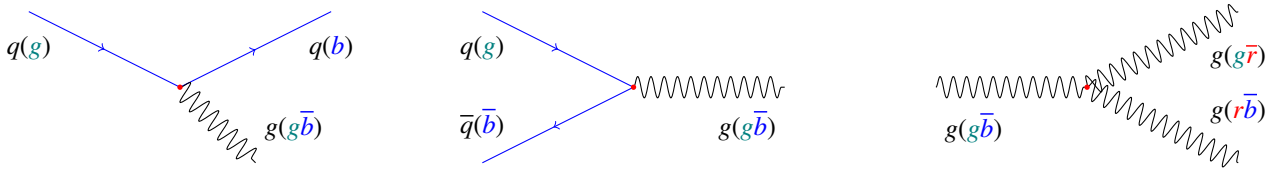
$$\frac{N(\text{3-jet})}{N(\text{2-jet})} \approx 0.15 \quad \text{at } \sqrt{s} \approx 20 \text{ GeV}.$$

Four-jet events are also important as they come from the self-interaction of the gluon as it splits.



5.1 Introduction to QCD

Quantum ChromoDynamics proposes that quarks carry one of three colour charges (labelled: *red, green, blue*) in addition to, and independent of, their fractional electric charge. In reciprocation, antiquarks carry anticolour charge (labelled: *red-bar, green-bar, blue-bar*). Strong force interactions occur by the exchange of massless electrically-neutral bosons called *gluons*. In contrast to the electromagnetic force carrier (the photon), gluons carry a mix of colour-charges and thus can couple to themselves as well as to quarks. Some examples of colour-conserving strong interactions are,



Unlike the photon, which has infinite range, the strong force effect is confined to within hadrons and cannot be sensed directly. The strong force potential for a $q\bar{q}$ bound state is modelled with two parts,

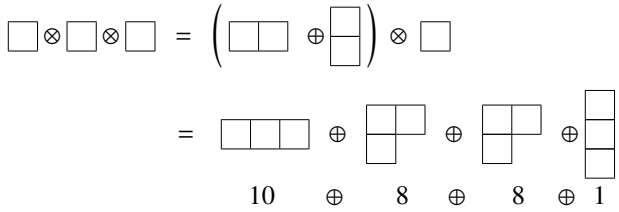
$$V(r) = -C\frac{\alpha_s}{r} + \lambda r \tag{49}$$

where C is the *colour factor* (see later), α_s is the strong coupling constant and $\lambda \sim 1\,\mathrm{GeV/fm}$. If the colour factor is negative, the first term becomes reminiscent of a Coulomb potential; this is justified by, e.g. the observed quarkonia spectra. The second term is a simple model of the confining potential. As the $\pi\pi$ invariant mass around 270 MeV/c^2, the gluon field will find it energetically favourable to pair-produce hadrons rather than allow a free quark to escape a bound state (proton radius $\approx 0.8\,\mathrm{fm}$).

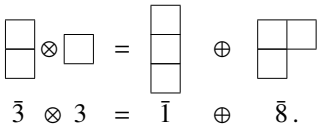
The three charges of QCD respect the SU(3) symmetry exactly. This is contrast to the broken SU(3) symmetry in the flavour structure of u, d, s mesons and baryons in the *Basics* lectures. Mathematically, this means that the strong interaction is invariant under rotation in colour space. Or practically speaking, that there is no way of telling which charge any given quark is carrying.

In the *Basics* lectures, Young's tableaux are used to combine three SU(3) particles and a SU(3) particle-antiparticle pair,

Baryons :



Mesons :



In each case a colour singlet occurs which defines the colour wavefunctions,

- Baryons: $\frac{1}{\sqrt{6}}(rgb - rbg + gbr - grb + brg - bgr)$ Antisymmetric wavefunction
- Mesons: $\frac{1}{\sqrt{3}}\left(r\bar{r} + g\bar{g} + b\bar{b}\right)$ Symmetric wavefunction

which are the same for all mesons and baryons. Note that other colour-neutral combinations, e.g. $\frac{1}{\sqrt{2}}(r\bar{r} - g\bar{g})$, which one might identify as the SU(3) colour analogy of the π^0, is not colourless as it is part of the octet (like the π^0). The singlet states colourless in the sense that when applying either raising or lowering operators, the wavefunction vanishes.

An exchange of gluons will rotate the colour state. The Gell-Mann basis is common, it is built on (and contains) the Pauli spin matrices. It extends the idea of raising and lowering between "spin $\frac{1}{2}$" and "spin $-\frac{1}{2}$" with a third degree. Imagine

moving around a triangle rather than just up and down. The Gell-Mann basis is defined as $T_i = \frac{1}{2}\lambda_i$ where, the first three SU(3) basis matrices are those of SU(2),

$$\lambda_1 = \begin{pmatrix} 0 & 1 & 0 \\ 1 & 0 & 0 \\ 0 & 0 & 0 \end{pmatrix} \quad \lambda_2 = \begin{pmatrix} 0 & -i & 0 \\ i & 0 & 0 \\ 0 & 0 & 0 \end{pmatrix} \quad \lambda_3 = \begin{pmatrix} 1 & 0 & 0 \\ 0 & -1 & 0 \\ 0 & 0 & 0 \end{pmatrix}$$

The SU(2) basis can be applied between the 1st and 3rd element,

$$\lambda_4 = \begin{pmatrix} 0 & 0 & 1 \\ 0 & 0 & 0 \\ 1 & 0 & 0 \end{pmatrix} \quad \lambda_5 = \begin{pmatrix} 0 & 0 & -i \\ 0 & 0 & 0 \\ i & 0 & 0 \end{pmatrix} \quad \lambda_a = \begin{pmatrix} 1 & 0 & 0 \\ 0 & 0 & 0 \\ 0 & 0 & -1 \end{pmatrix}$$

And again between the 2nd and 3rd elements,

$$\lambda_6 = \begin{pmatrix} 0 & 0 & 0 \\ 0 & 0 & 1 \\ 0 & 1 & 0 \end{pmatrix} \quad \lambda_7 = \begin{pmatrix} 0 & 0 & 0 \\ 0 & 0 & -i \\ 0 & i & 0 \end{pmatrix} \quad \lambda_b = \begin{pmatrix} 0 & 0 & 0 \\ 0 & 1 & 0 \\ 0 & 0 & -1 \end{pmatrix}$$

We note that the three diagonal matrices, λ_3, λ_a and λ_b are not independent, $\lambda_3 = \lambda_a - \lambda_b$. So choose to keep λ_3 as-is and make an orthogonal combination of the other two,

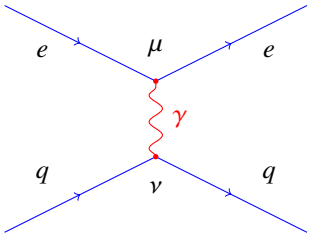
$$\lambda_8 = \frac{1}{\sqrt{3}}[\lambda_a + \lambda_b] = \frac{1}{\sqrt{3}} \begin{pmatrix} 1 & 0 & 0 \\ 0 & 1 & 0 \\ 0 & 0 & -2 \end{pmatrix}$$

These are the eight traceless matrices expected from $\dim[\mathrm{SU}(n)] = n^2 - 1$.

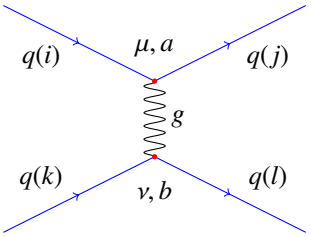
Each QCD exchange is a colour-conserving linear superposition of these eight, orthogonal gluons.

5.2 Comparison of the electron-quark (QED) and quark-quark (QCD) interaction

The lowest-order QCD matrix element is built by analogy to the lowest-order QED interaction in the derivation of Eq. 5. The modification for QCD takes into account the three possible colour charges of each quark ($i = 1, 2, 3$) and the eight possible gluons that connect them ($a, b = 1 : 8$).



QED



QCD

	QED	QCD
propagator	$-ig_{\mu\nu}/q^2$	$-i\delta^{ab}g_{\mu\nu}/q^2$
vertex factor	$ig_e\gamma^\mu$	$ig_s\gamma^\mu\lambda^a_{ji}/2$
coupling constant	$g_e = \sqrt{4\pi\alpha}$	$g_s = \sqrt{4\pi\alpha_s}$

The modifications with respect to the QED matrix element are highlighted.

- The delta function in the propagator, δ^{ab} requires the gluon charge at each vertex to be the same.
- The Gell-Mann matrices, λ^a_{ji} in the vertex term defines the probability of gluon a connecting colour charges i and j.
- The strength of the QCD coupling is governed by α_s which is 1-2 orders of magnitude larger than the QED coupling.

The lowest-order QCD quark-quark scattering matrix element is built in the same way as for the QED scattering,

$$-i\mathcal{M}_{fi} = \int \left[\bar{u}(p_3)\, ig_s\gamma^\mu \frac{\lambda^a_{ji}}{2} u(p_1)\right] \frac{-i\delta^{ab} g_{\mu\nu}}{q^2} \left[\bar{u}(p_4)\, ig_s\gamma^\nu \frac{\lambda^b_{lk}}{2} u(p_2)\right] \delta^4(p_1 - p_3 - q)\, d^4q\,.$$

$$\mathcal{M}_{fi} = -\frac{\lambda^a_{ji}\lambda^a_{lk}}{4} \frac{{g_s}^2}{(p_1 - p_3)^2} \left[\bar{u}(p_3)\,\gamma^\mu\, u(p_1)\right]\left[\bar{u}(p_4)\,\gamma_\mu\, u(p_2)\right],$$

which is identical to the QED case except for the coupling strength and a *colour factor* from the Gell-Mann matrices.

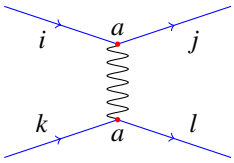
5.3 Colour factors

The colour factor is thus defined for quark-quark scattering for $a = \{1-8\}$ and $i, j = \{1, 2, 3\}$,

$$C = \frac{1}{4}\sum_a \lambda^a_{ji}\,\lambda^a_{lk} \tag{50}$$

Next we calculate the colour factors for three types of colour exchange from inspection of the Gell-Mann basis matrices,

$i = j = k = l$

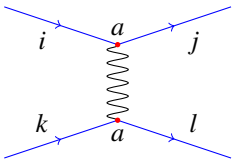


$rr \to rr$ $\quad \frac{1}{4}\left(\lambda^3_{11}\lambda^3_{11} + \lambda^8_{11}\lambda^8_{11}\right) = \frac{1}{4}\left(1\cdot 1 + \frac{1}{\sqrt{3}}\frac{1}{\sqrt{3}}\right)$

$gg \to gg$ $\quad \frac{1}{4}\left(\lambda^3_{22}\lambda^3_{22} + \lambda^8_{22}\lambda^8_{22}\right) = \frac{1}{4}\left(-1\cdot -1 + \frac{1}{\sqrt{3}}\frac{1}{\sqrt{3}}\right)$ $\quad$ all $= +\frac{1}{3}$

$bb \to bb$ $\quad \frac{1}{4}\left(\lambda^8_{33}\lambda^8_{33}\right) = \frac{1}{4}\left(\frac{-2}{\sqrt{3}}\frac{-2}{\sqrt{3}}\right)$

$i = j\,,\ k = l$

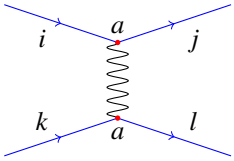


$rg \to rg$, $gr \to gr$ $\quad \frac{1}{4}\left(\lambda^3_{11}\lambda^3_{22} + \lambda^8_{11}\lambda^8_{22}\right) = \frac{1}{4}\left(1\cdot -1 + \frac{1}{\sqrt{3}}\frac{1}{\sqrt{3}}\right)$

$rb \to rb$, $br \to br$ $\quad \frac{1}{4}\left(\lambda^8_{11}\lambda^8_{33}\right) = \frac{1}{4}\left(\frac{1}{\sqrt{3}}\frac{-2}{\sqrt{3}}\right)$ $\quad$ all $= -\frac{1}{6}$

$gb \to gb$, $bg \to bg$ $\quad \frac{1}{4}\left(\lambda^8_{22}\lambda^8_{33}\right) = \frac{1}{4}\left(\frac{1}{\sqrt{3}}\frac{-2}{\sqrt{3}}\right)$

$i = l\,,\ j = k$



$rg \to gr$, $gr \to rg$ $\quad \frac{1}{4}\left(\lambda^1_{12}\lambda^1_{21} + \lambda^2_{12}\lambda^2_{21}\right) = \frac{1}{4}\left(1\cdot 1 - i\cdot i\right)$

$rb \to br$, $br \to rb$ $\quad \frac{1}{4}\left(\lambda^4_{13}\lambda^4_{31} + \lambda^5_{13}\lambda^5_{31}\right) = \frac{1}{4}\left(1\cdot 1 - i\cdot i\right)$ $\quad$ all $= +\frac{1}{2}$

$gb \to bg$, $bg \to gb$ $\quad \frac{1}{4}\left(\lambda^6_{23}\lambda^6_{32} + \lambda^7_{23}\lambda^7_{32}\right) = \frac{1}{4}\left(1\cdot 1 - i\cdot i\right)$

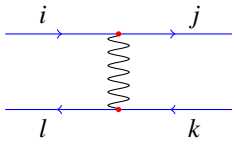
All other combinations will not be colour conserving so the colour factor is zero. A non-colour-conserving example:

$$C(rg \to gb) = \tfrac{1}{4}\textstyle\sum_a \lambda^a_{12}\lambda^a_{23} \;=\; \tfrac{1}{4}\left(1\cdot 0 - i\cdot 0 + 0\cdot 0 + 0\cdot 0 + 0\cdot 0 + 0\cdot 1 + 0\cdot i + 0\cdot 0\right) = 0\,.$$

For quark-antiquark interactions, the same factors come out of the Gell-Mann matrices, though with labels k and l swapped as the antiquark colour current is traveling backwards in time. The colour factors thus apply to the following colour-anticolour currents moving forward in time.

In a meson, the bound $q\bar{q}$ state must be colourless so the second group are not present. The colour factor in the meson potential of Eq. 49, averaged over the three possible colour-anticolour combinations is,

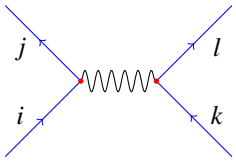
$$C(q\bar{q})_{\text{meson}} = \frac{1}{3}\left(3\cdot\frac{1}{3} + 6\cdot\frac{1}{2}\right) \;=\; \frac{4}{3}\,.$$



$C = +\frac{1}{3}$: $r\bar{r} \to r\bar{r}$, $g\bar{g} \to g\bar{g}$, $b\bar{b} \to b\bar{b}$

$C = -\frac{1}{6}$: $r\bar{g} \to r\bar{g}$, $r\bar{b} \to r\bar{b}$, $g\bar{r} \to g\bar{r}$, $g\bar{b} \to g\bar{b}$, $b\bar{r} \to b\bar{r}$, $b\bar{g} \to b\bar{g}$

$C = +\frac{1}{2}$: $r\bar{r} \to g\bar{g}$, $r\bar{r} \to b\bar{b}$, $g\bar{g} \to r\bar{r}$, $g\bar{g} \to b\bar{b}$, $b\bar{b} \to r\bar{r}$, $b\bar{b} \to g\bar{g}$



$C = +\frac{1}{3}$: $r\bar{r} \to r\bar{r}$, $g\bar{g} \to g\bar{g}$, $b\bar{b} \to b\bar{b}$

$C = -\frac{1}{6}$: $r\bar{r} \to g\bar{g}$, $r\bar{r} \to b\bar{b}$, $g\bar{g} \to r\bar{r}$, $g\bar{g} \to b\bar{b}$, $b\bar{b} \to r\bar{r}$, $b\bar{b} \to g\bar{g}$

$C = +\frac{1}{2}$: $r\bar{g} \to \bar{g}r$, $r\bar{b} \to \bar{b}r$, $g\bar{r} \to \bar{r}g$, $g\bar{b} \to \bar{b}g$, $b\bar{r} \to \bar{r}b$, $b\bar{g} \to \bar{g}b$

For the s-channel, quark-anitquark annihilation process, the same three colour factors are used but i and j label the initial state, k and l the final state. To calculate a cross section we must sum over possible colour exchange amplitudes (squared) and average over the possible initial colour states of the colliding quarks ($3 \times 3 = 9$ colour combinations). The colour factors and the number of exchanges they refer to are listed above. So for $q\bar{q}$ annihilation the total colour factor is,

$$|C(q\bar{q} \to q\bar{q})|^2 = \frac{1}{9}\left(3\left|+\frac{1}{3}\right|^2 + 6\left|-\frac{1}{6}\right|^2 + 6\left|+\frac{1}{2}\right|^2\right) = \frac{2}{9}.$$

With these factors calculated, we borrow from $eq \to eq$ differential cross section, Eq. 19, we postulate a lowest-order differential cross section for $q\bar{q} \to q\bar{q}$ where the QCD modifications are highlighted,

$$\frac{d\sigma}{dq^2} = -\frac{2}{9}\frac{4\pi{\alpha_s}^2}{q^4}\left[1 - y + \frac{y^2}{2}\right]. \tag{51}$$

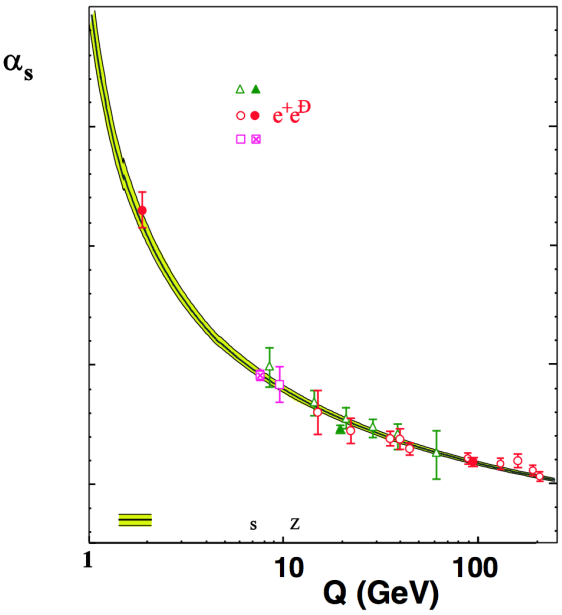
In experimental tests of QCD scattering, e.g. $p\bar{p}$ collisions at the Tevatron, such cross section calculations are repeated for all categories of parton collision ($q\bar{q}$, qg, $\bar{q}g$, gg) and to NNLO accuracy; excellent agreement with the data is seen.

5.4 Running coupling constant

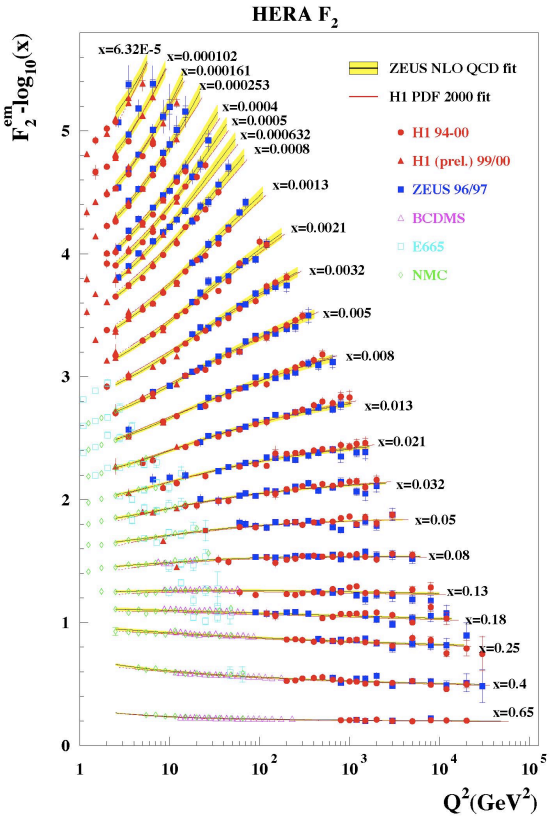
The QED coupling constant, α is known to strengthen at high Q^2 where the distances scales reduce and a probe charge can approach more closely the target charge. At short distances the QED screening that dilutes the bare charge strength, diminishes and the true bare charge becomes more apparent. $\alpha = \frac{1}{137}$ at low energies and rises to $\alpha = \frac{1}{128}$ around 170 GeV. In QCD, because the gluons self-interact, there is screening but there is a more-powerful anti-screening effect. that enhances the colour charge strength at large distances. At progressively higher energies (shorter distance scales) the strength of the strong coupling diminishes. This effect can only arrise from a self-interacting field, as required by QCD. The magnitude of α_s as shown on the plot is predicted to be,

$$\alpha_s(Q^2) = \frac{\alpha_s(\Lambda)}{1 + \alpha_s(\Lambda)\frac{11N_c - 2N_f}{12\pi}\ln\left(\frac{q^2}{\Lambda}\right)},$$

where N_c and N_f are the number of charges and the number of quark flavours in the theory and $\Lambda \approx 300$ MeV.



6 Modern PDFs and their application



Scaling violations

For a photon to resolve structure, its wavelength must be as least as small as that structure. From,

$$\lambda = \frac{\hbar}{|\underline{q}|} = \frac{197\ \text{MeV fm}}{|\underline{q}|\,[\,\text{MeV}/c]c}$$

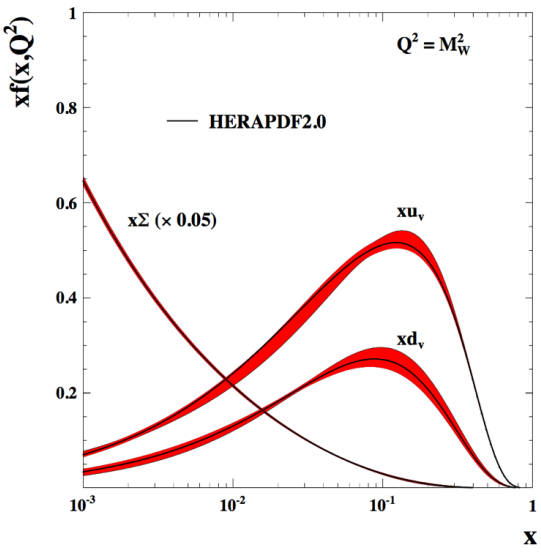
we see that the energy to resolve the proton structure (1 fm) needs $|\underline{q}| \approx 200$ MeV and the energy to resolve quark structure (10^{-18}m) is $|\underline{q}| \approx 200$ GeV. The smallest distance scales were probed by the HERA facility that operated near Hamburg in the 1990s and 2000s, colliding $e^- p$ at $\sqrt{s} \approx 300$ GeV. The accumulated F_2 structure function data is shown in the plot and these data show Blorken scaling down to momentum fractions $x > 0.05$. However, at lower x, increasingly the Bjorken-scaling seems violated, but not in a manner that is consistent with quark structure (rapid decrease in structure with Q^2). Rather, the electron probe sees increasing structure at larger Q^2 for the smallest x!

QCD can explain this as follows: at low x the proton is all gluons and sea quarks flashing into existence for a short period. For this short period, the electron probe can scatter off the charged quark or antiquark. At higher Q^2 the distance (and thus time) scales that the the electron can probe gets smaller, so the more short-lived $q\bar{q}$ pairs are visible, thus more scattering occurs and the measured structure function rises. The data shows excellent agreement with the QCD prediction.

Understanding of the proton structure at low-x has been critical in predicting and understanding the LHC cross sections. As the LHC is a proton-proton collider, there are no valance anti-quarks to collide. The LHC is entirely reliant on the gluons and sea-quarks for every LHC collision. Studies of the proton structure is critical to the success of the LHC.

PDF fits

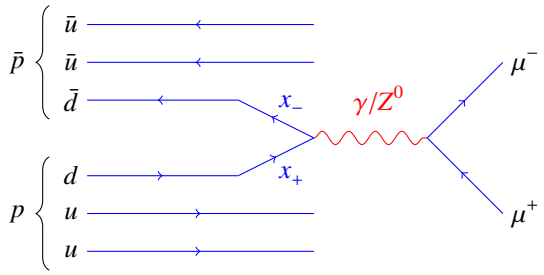
The modern representation of the proton structure shows the structure function versus Bjorken-x for each component of the proton. One scuh summary is shown here; it is derived from the HERAPDF model fitted to all deep inelastic scattering data. The red band shows the fit uncertainty.
As the influence of the sea quarks comes in a small x, the PDFs are shown along on a logarithmic scale. The integral of each component PDF is, nevertheless, the total fraction of the four-momentum carried by that parton.
From the plot we see that the integral of the up quark PDF about twice that of the down quark and has a marginally harder momentum spectrum.
The sea quark PDF rises rapidly at low x. Their PDFs are summed together $\mathbf{\Sigma = 2(\bar{u}(x) + \bar{d}(x) + \bar{s}(x) + \bar{c}(x))}$. The result is graphically scaled by $^1/_{20}$ to fit on the plot.



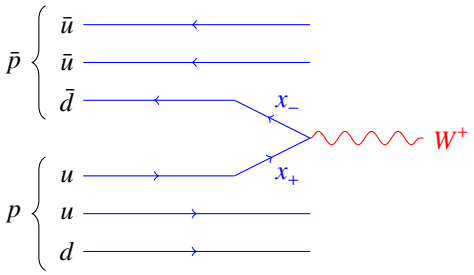
xFitter (2018), Cooper-Sarkar.

6.1 proton-antiproton cross sections

The understanding of the proton structure is used in the calculation of cross sections at hadron colliders. In the case of the Tevatron, which collided protons and antiprotons at $\sqrt{s} = 2$ TeV until 2009, two important processes are studied in detail. The colliding quarks will have momentum share , x_+ and x_- in the proton and antiproton respectively. Where the quarks are of the same flavour, a neutral boson exchange with the final state occurs. This is most readily studies with dimuon production as there are no leptons in the initial state. Where the quarks are of different flavour, $W^\pm$ boson production occurs.



Drell-Yan production from $p\bar{p}$ collisions



Production of $W^\pm$ from $p\bar{p}$ collisions

The CoM-energy-squared, $(p_p + p_{\bar{p}})^2 \approx 2p_p \cdot p_{\bar{p}} = s$, and neglecting any transverse component, the two colliding quarks have 4-momentum,

$$p_+ = \frac{\sqrt{s}}{2}(x_+,\, 0\,,\, 0\,,\, x_+) \qquad p_- = \frac{\sqrt{s}}{2}(x_-,\, 0\,,\, 0\,,\, -x_-)$$

The energy and [longitudinal] momentum of the quark-antiquark collision is,

$$E_{q\bar{q}} = \frac{\sqrt{s}}{2}(x_+ + x_-)\,, \quad |\mathbf{p}_{q\bar{q}}| = \frac{\sqrt{s}}{2}(x_+ - x_-)\,. \quad \text{Thus the invariant mass,} \quad M^2_{q\bar{q}} = x_+x_-s\,, \text{and the rapidity, } y,$$

$$y = \frac{1}{2}\ln\left(\frac{E+\mathbf{p}_z}{E-\mathbf{p}_z}\right) = \frac{1}{2}\ln\left(\frac{x_+}{x_-}\right) \quad \text{or} \quad \frac{x_+}{x_-} = e^{2y}\,.$$

A simple rearrangements relates the rapidity to Bjorken-x,

$$\frac{(x_+)^2 s}{M^2_{q\bar{q}}} = e^{2y} \quad \Rightarrow \qquad x_+ = \sqrt{\tau}e^{+y}\,.$$

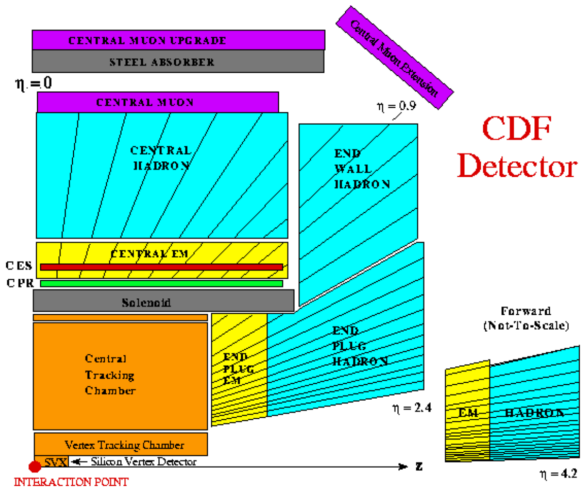
$$\frac{M^2_{q\bar{q}}}{(x_-)^2 s} = e^{2y} \quad \Rightarrow \qquad x_- = \sqrt{\tau}e^{-y}\,.$$

where a variable $\tau = \frac{M^2_{q\bar{q}}}{s}$ is introduced; $\sqrt{\tau}$ is the fraction of the total CoM energy in the $q\bar{q}$ collision.

The CDF detector at the Tevatron instruments the central region of the $p\bar{p}$ collisions with rapidity range $-2 < y < 2$. From the above relations, the range of assessable Bjorken-x that the CDF detector can study is calculated.

y	-2	-1	0	1	2
x_+	0.005	0.015	0.040	0.109	0.297
x_-	0.297	0.109	0.040	0.015	0.005

if one considers $W^\pm$ production: $M_{q\bar{q}} = m_W = 80.35$ GeV/c^2.



A cutaway showing one quarter of the CDF detector. The tracker covers pseudorapidity $|\eta| < 2.4$ ($\eta \simeq y$).

Example: $W^\pm$ production asymmetry at the Tevatron

As there is a direct relationship between Bjorken-x and rapidity,

$$\frac{d\sigma(W^\pm)}{dy} = \frac{dx+\pm}{dy}\frac{d\sigma(W^+)}{dx_\pm} = \pm\sqrt{\tau}e^{\pm y}\left.\frac{d\sigma}{dx_\pm}\right|_{Q^2=m_w^2}$$

Thus an expression for differential cross section can be,

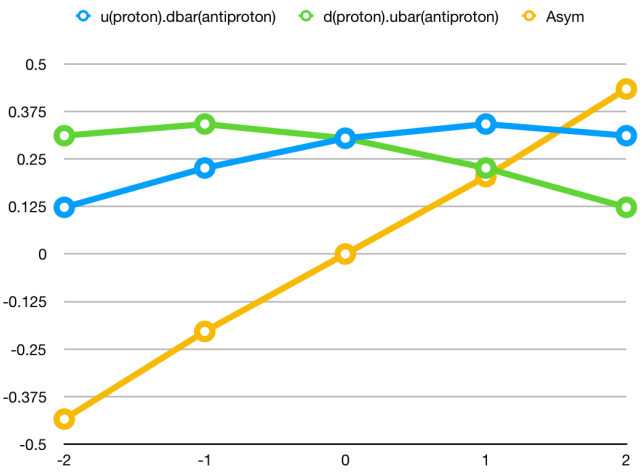
$$\frac{d\sigma(W^+)}{dy} \propto \left[u^p(x_+)\,\bar{d}^{\bar{p}}(x_-) + \cancel{\bar{d}^p(x_+)\,u^{\bar{p}}(x_-)}\right] = \left[u_{\text{val}}(x_+) + u_{\text{sea}}(x_+)\right]\left[\bar{d}_{\text{val}}(x_-) + \bar{d}_{\text{sea}}(x_-)\right],$$

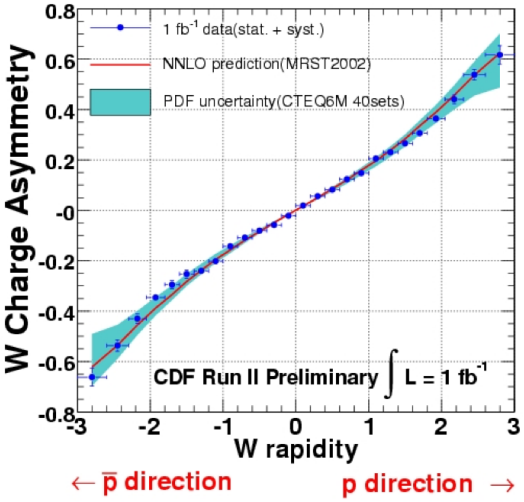
$$\frac{d\sigma(W^-)}{dy} \propto \left[d^p(x_+)\,\bar{u}^{\bar{p}}(x_-) + \cancel{\bar{u}^p(x_+)\,d^{\bar{p}}(x_-)}\right] = \left[d_{\text{val}}(x_+) + d_{\text{sea}}(x_+)\right]\left[\bar{u}_{\text{val}}(x_-) + \bar{u}_{\text{sea}}(x_-)\right],$$

The first term in each expression is dominated by the valance quarks at high x but the sea quarks must be included at low x. The second term describes both partons coming from sea. As one of the partons always has high x, this term can be neglected and we continue with first term only.

In this demonstration, we can simple read off $u_v(x)$, $d_v(x)$ and $\Sigma(x)$ for each x_+ and x_-, remembering to divide the $\Sigma(x)$ by eight to get the individual quark or antiquark contribution. The final line (marked with an *) is proportional to the differential cross section. The equivalent PDF numbers for W^- are the same, but reverse across the row, from the symmetry of $p\bar{p} \to W^{\pm}X$ production. These numbers are sketched below and an asymmetry and from which an asymmetry can be seen. This asymmetry, studied at CDF, is shown in the plot.

y	-2	-1	0	1	2	
x_+	0.005	0.015	0.040	0.109	0.297	
xu_v (valance)	0.17	0.28	0.43	0.52	0.36	
$x\Sigma/8$ (sea)	0.78	0.45	0.23	0.05	0.00	
$u^p(x_+) = x(u_v + \Sigma/8)$	0.95	0.73	0.66	0.57	0.36	
x_-	0.297	0.109	0.040	0.015	0.005	
xd_v (valance)	0.13	0.26	0.24	0.15	0.09	
$x\Sigma/8$ (sea)	0.00	0.05	0.23	0.45	0.78	
$\bar{d}^p(x_-) = x(d_v + \Sigma/8)$	0.13	0.31	0.47	0.60	0.87	
W^+: $u^p(x_+)\,\bar{d}^p(x_-)$	0.123	0226	0.305	0.342	0.311	*





The backward-forward asymmetry, the humped peaking structure and the fact that the W^+ distribution peaks in positive rapidity, vice-versa for W^- production. The blue data point at from $p\bar{p}$ collisions and shows excellent agreement with the prediction from the PDF fits to deep inelastic scattering data (red line).

Example: $W^{\pm}$ production asymmetry at the LHC

As the LHC collides is a pp, rather than a $p\bar{p}$ collider, the initial state is forward-backward symmetric so a large variation in the $W^{\pm}$ production asymmetry, as seen at the Tevatron is not expected. However, the dominance of u_{valance} over d_{valance} means that one expects to produce more W^+ than W^-.

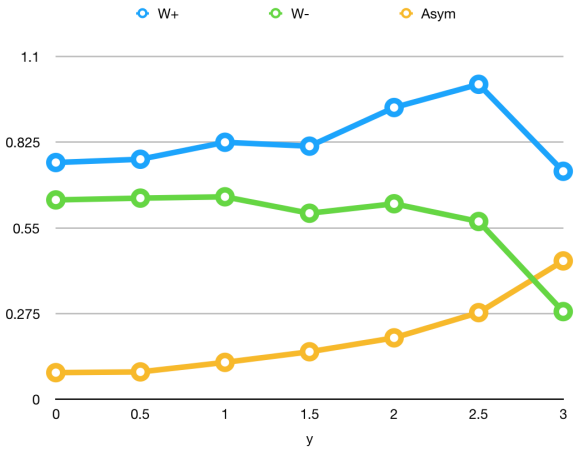
Labelling the first proton's momentum fraction x_1 and the second's x_2, an expression for differential cross section for the $p\bar{p}$ case, in which we must use sea-quarks in both expressions,

$$\frac{d\sigma(W^+)}{dy} \propto [u_{\text{val}}(x_1) + u_{\text{sea}}(x_1)]\ \bar{d}_{\text{sea}}(x_2) \ + \ \bar{d}_{\text{sea}}(x_1)\ [u_{\text{val}}(x_2) + u_{\text{sea}}(x_2)]\ ,$$

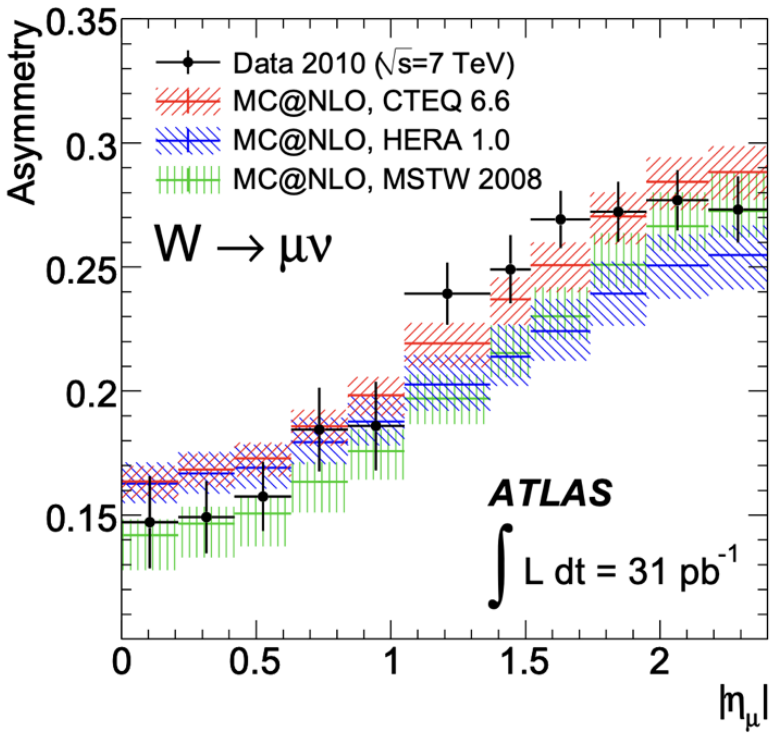
$$\frac{d\sigma(W^-)}{dy} \propto [d_{\text{val}}(x_1) + d_{\text{sea}}(x_1)]\ \bar{u}_{\text{sea}}(x_2) \ + \ \bar{u}_{\text{sea}}(x_1)\ [d_{\text{val}}(x_2) + d_{\text{sea}}(x_2)]\ ,$$

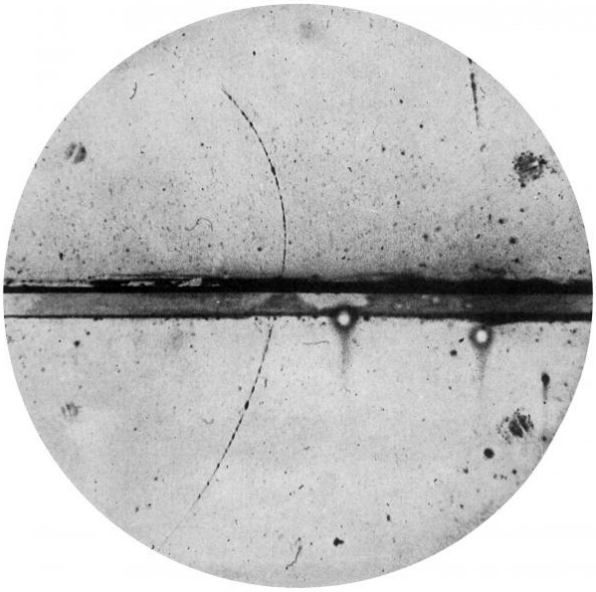
Running through a similar exercise for $\sqrt{s}(pp)$ = 7TeV and $0 < |y| < 2.5$, again reading the value off the PDF plot,

y	0	1	2	3
x_+	0.011	0.031	0.085	0.231
xu_v (valance)	0.26	0.40	0.50	0.30
xd_v (valance)	0.14	0.22	0.27	0.10
$x\Sigma/8$ (sea)	0.50	0.25	0.10	0.01
x_-	0.011	0.004	0.002	0.001
xu_v (valance)	0.26	0.15	0.09	0.05
xd_v (valance)	0.14	0.08	0.05	0.03
$x\Sigma/8$ (sea)	0.50	0.88	1.33	2.25
W^+:	0.76	0.83	0.94	0.73
W^-:	0.64	0.65	0.63	0.28



one see an asymmetry varying as a function of y but aways positive (as expected) with an average of around 0.33 (again, as epected) This pattern is also seen in data, as seen in the following ATLAS/LHC result at $\sqrt{s}$ = 7TeV.





The Oxford MPhys Course

C4: Particle Physics

Problem Set Five

1. Consider scattering from an extended spherical charge distribution (e.g. electron scattering from a nucleus):

$$V(r) = g^2 \int \frac{\rho(r')\mathrm{d}^3\vec{r'}}{|\vec{r} - \vec{r'}|}, \qquad \text{where} \qquad \int \rho(r')\mathrm{d}^3\vec{r'} = 1.$$

The Fourier transform of the potential is

$$U(q^2) = g^2 \int \frac{\rho(r')\mathrm{e}^{\mathrm{i}\vec{q}\cdot\vec{r}}}{|\vec{r} - \vec{r'}|}\mathrm{d}^3\vec{r'}\mathrm{d}^3\vec{r}.$$

(a) Show that by introducing the variable $\vec{R} = \vec{r} - \vec{r'}$ one may write (after two angular integrations)

$$U(q^2) = \frac{2\pi g^2 F(q^2)}{\mathrm{i}q} \int_0^\infty \left(\mathrm{e}^{\mathrm{i}qR} - \mathrm{e}^{-\mathrm{i}qR}\right) \mathrm{d}R,$$

where $F(q^2) = \int \rho(r')\mathrm{e}^{\mathrm{i}\vec{q}\cdot\vec{r'}}\mathrm{d}^3\vec{r'}$ is the Fourier transform, or *form factor*, of the charge distribution.

(b) The remaining radial integral in the expression for $U(q^2)$ is divergent as it stands, but it can be performed by introducing an extra factor $\mathrm{e}^{-\mu R}$ under the integral

©University of Oxford 2022

and taking the limit $\mu \to 0$ afterwards. Show that the end result is

$$U(q^2) = \frac{4\pi g^2}{q^2} F(q^2).$$

(c) The change from a point-like to an extended scattering centre is a multiplication of the point-like amplitude by the form factor $F(q^2)$. Equivalently, the point-like (Rutherford) cross-section is modified by the term $|F(q^2)|^2$.

From elastic electron-proton scattering, the form factor is well described by the simple expression $F(q^2) = (1 + q^2/0{\cdot}71)^{-2}$, where q^2 is measured in $(\mathrm{GeV}/c)^2$. Using this information and the expression for $F(q^2)$ in terms of $\rho(r)$ above, approximated for small q^2, estimate the mean square radius of the proton. The mean square radius $\langle r'^2 \rangle$ of a distribution $\rho(\vec{r'})$ is given by

$$\langle r'^2 \rangle = \int r'^2 \rho(\vec{r'}) \mathrm{d}^3\vec{r'}.$$

[In this problem, proton recoil has been ignored, and the problem posed in terms of the 3-momentum transfer $\vec{q}$ rather than more precisely in terms of the 4-momentum transfer that will be used in deep inelastic scattering. These complications do not change the essence of the physical ideas.]

2. The first-order QED differential cross-section for elastic $e\mu$ scattering,

$$e(k) + \mu(p) \to e(k') + \mu(p'),$$

where k, k', p, p' are four-vectors, is:

$$\frac{d\sigma}{dy} = \frac{2\pi\alpha^2 \hat{s}}{Q^4}[1 + (1-y)^2].$$

In this expression, $\hat{s} = (p+k)^2$ is the total centre-of-mass energy squared, $Q^2 = -q^2 = -(k-k')^2$ is the negative four-momentum transfer squared, and $y = p{\cdot}q/p{\cdot}k$.

(a) Show that in the high-energy limit y is simply related to θ^*, the scattering angle in the $e\mu$ centre-of-mass frame. Discuss the physics of the formula for $d\sigma/dy$.

(b) In the parton model of the nucleon, the differential cross-section for charged lepton-nucleon scattering is given by,

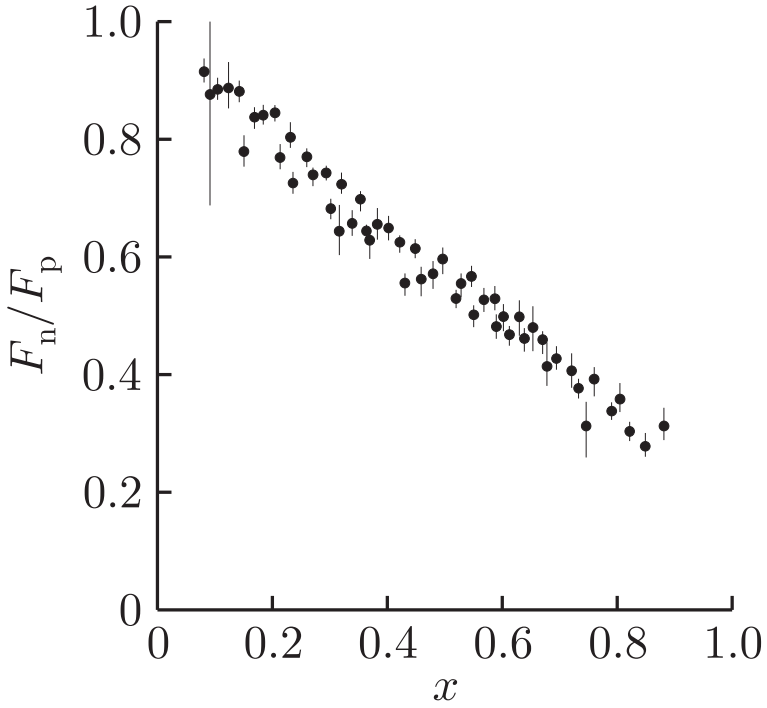
$$\frac{d^2\sigma}{dxdy} = \frac{2\pi\alpha^2 s}{Q^4}[1 + (1-y)^2]F_2(x),$$

where $x = Q^2/(2q{\cdot}P)$, with P the nucleon four-momentum and $\sqrt{s}$ the lepton-nucleon centre-of-mass energy. Explain the assumptions made in deriving this result from the point-like scattering cross-section. Interpret $F_2(x)$.

(c) Express the structure functions $F_2^p(x)$ and $F_2^n(x)$ for the proton and the neutron, respectively, in terms of quark and anti-quark distribution functions $u, d, s, \bar{u}, \bar{d}$, and $\bar{s}$, where $u \equiv u(x)$ and equivalently for all others.

©University of Oxford 2022

(d) The figure below shows the ratio $F_2^n(x)/F_2^p(x)$ as a function of x. What does the data imply about the relative importance of 'valence' and 'sea' quarks as a function of x (ignoring s and $\bar{s}$ contributions)?



3. Use the simple parton-model expressions for F_2^p and F_2^n in terms of the quark distributions from the previous question, to discuss the following:

(a) What do the integrals $\int_0^1 F_2^n(x)dx = 0{\cdot}12$ and $\int_0^1 F_2^p(x)dx = 0{\cdot}18$ say about the constituents carrying the nucleon's momentum? Assume the strange quark contributions are small.

(b) $F_2^p - F_2^n$ peaks around $x \approx 0{\cdot}35$ and $\displaystyle\int_0^1 (F_2^p - F_2^n)\frac{dx}{x} = 0{\cdot}235 \pm 0{\cdot}026$. Is the integral consistent with a 'flavour symmetric' sea, and, if not, what are the implications?

(c) The figure shows F_2^p values as functions of Q^2 for bins of fixed x. Only for $x > 0{\cdot}05$ does the data exhibit approximate Bjorken scaling (F_2 independent of Q^2). Outline how the behaviour at low x may be understood in terms of quark and gluon interactions described by QCD.

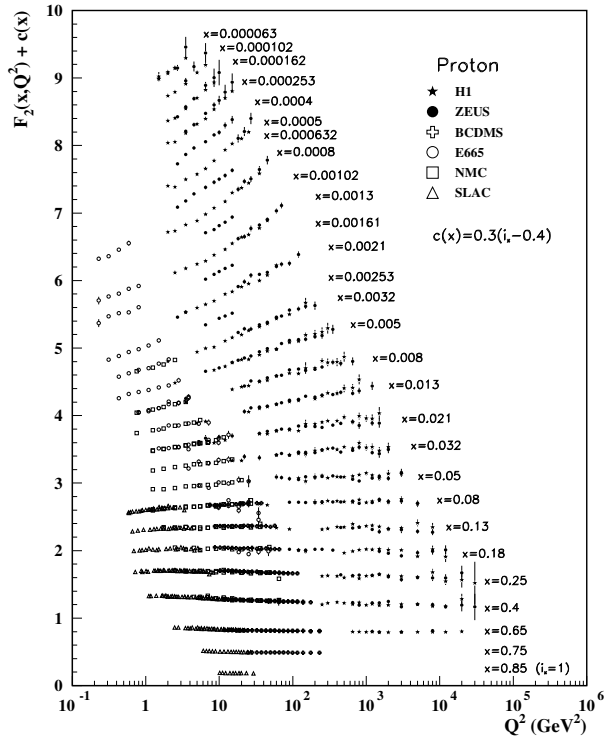


Figure. $F_2(x, Q^2)$ vs Q^2 at fixed x values. Note that there is an arbitrary offset c applied to each data set at a given x in order to increase the visibility.

4. Deep inelastic charged-current scattering of muon neutrinos by an isoscalar target is the process

$$\nu(k) + \mathrm{N}(p) \;\rightarrow\; \mu^-(k') + \mathrm{X}(p_\mathrm{X}),$$

where 4-momenta are indicated by the symbols in the brackets and X represents the hadronic final state. For centre-of-mass energies in the range $m_\mathrm{N} \ll \sqrt{s} \ll M_\mathrm{W}$, the double-differential cross-section may be written in terms of the parton momentum density functions (PDFs) of the proton as

$$\frac{\mathrm{d}^2\sigma}{\mathrm{d}x\mathrm{d}y} = \frac{s{G_\mathrm{F}}^2}{2\pi} x\left[d(x) + u(x) + (1-y)^2(\bar{u}(x) + \bar{d}(x))\right] ,$$

where $q = k - k'$, $Q^2 = -q^2$, $x = \dfrac{Q^2}{2p\cdot q}$, $y = \dfrac{p\cdot q}{p\cdot k}$, and G_F is the Fermi constant.

(a) Give a brief account of the assumptions underlying the above formula and the origin of the y dependence.

(b) Only u, d, $\bar{\mathrm{u}}$, $\bar{\mathrm{d}}$ PDFs have been considered in the above expression. How do the strange sea $\bar{\mathrm{s}}\,\mathrm{s}$ PDFs enter the expression for the cross-section?

(c) What form does the corresponding double-differential cross-section take for $\bar{\nu}\mathrm{N} \rightarrow \mu^+\mathrm{X}$?

©University of Oxford 2022

(d) A high-energy νN (and $\bar{\nu}$N) scattering experiment is performed using a broad-band beam with $30 < E_\nu < 600\,\text{GeV}$ and mean energy of 160 GeV. The detector consists of a large iron-scintillator hadronic calorimeter, which also serves as the target, followed by a muon spectrometer consisting of drift chambers interspersed between toroidal bending magnets and iron absorber plates. Using this detector the following quantities may be measured:

(i) the energy E_μ of the muon;

(ii) the production angle θ_μ of the muon track with respect to the neutrino beam direction;

(iii) the energy E_X of the hadronic system.

Ignoring the muon mass, show that $Q^2 = 4E_\text{vis}E_\mu \sin^2(\theta_\mu/2)$, $y = E_\text{X}/E_\text{vis}$, where $E_\text{vis} = E_\text{X} + E_\mu$ and find an expression for x.

(e) The resolution of the calorimeter is $\sigma_E/E = 0{\cdot}87/\sqrt{E(\text{GeV})}$ and that of the muon spectrometer is $\sigma_E/E = 0{\cdot}11$. A νN event is reconstructed with $E_\text{X} = 95\,\text{GeV}$, $E_\mu = 65\,\text{GeV}$ and $\theta_\mu = 5^\circ$. Calculate the corresponding values of x and Q^2 and estimate the resolution with which they can be measured, assuming that the uncertainty in the measurement of θ_μ is negligible.

(f) Draw Feynman diagrams to show how charmed quarks may be produced in νN and $\bar{\nu}$N interactions. Explain, with appropriate diagrams and paying particular attention to the signs of the electric charges of the muons, how certain di-muon events may indicate charm production. Which of νN or $\bar{\nu}$N is likely to give the larger signal to background ratio and why?

5. At the HERA collider 27.5 GeV positrons collide with 820 GeV protons, and for large momentum transfers the charged-current (CC) process $e^+p \to \bar{\nu}_e X$ has been measured. Within the context of the quark-parton model (QPM), consider first the process

$$e^+(k) + q(p) \to \bar{\nu}_e(k') + q'(p'),$$

where the symbols in the brackets denote the 4-momenta of the particles and q and q' represent quarks (or antiquarks) in the initial and final states respectively.

(a) Confining consideration to quark flavours in the first two generations, and ignoring Cabbibo-suppressed couplings, draw Feynman diagrams for CC e^+q and $e^+\bar{q}$ processes.

(b) In the e^+q CM the angular distribution for CC scattering is given by:

$$\frac{d\sigma}{d\Omega} = \frac{\hat{s}G_F^2}{8\pi^2}\left(\frac{M_W^2}{M_W^2+Q^2}\right)^2 |d^J|^2,$$

where $\sqrt{\hat{s}}$ is the e^+q CM energy, $Q^2 = -q^2$, d^J is a rotation matrix and other symbols have their usual meaning. By considering helicity transfer in the e^+q CM, identify the appropriate elements of the d^J matrices for $e^+q \to \bar{\nu}_e q' X$ and $e^+\bar{q} \to \bar{\nu}_e \bar{q}'$.

(c) Using the forms for the parton-level processes derived from the above differential cross-section, justify the quark-parton-model expression for the $e^+p \to \bar{\nu}_e X$ double-differential cross-section,

$$\frac{d^2\sigma}{dxdy} = \frac{sG_F^2}{2\pi}\left(\frac{M_W^2}{M_W^2+Q^2}\right)^2 x\left[\bar{u}(x)+\bar{c}(x)+(1-y)^2(d(x)+s(x))\right],$$

where $\sqrt{s}$ is the e^+p centre-of-mass energy and $x = Q^2/2p{\cdot}q$, with $q = k - k'$, is the Bjorken scaling variable. The expression $y = \frac{1}{2}(1-\cos\theta^*)$ may be assumed, where $y = q{\cdot}p/k{\cdot}p$ and θ^* is the e^+q CM scattering angle. Pay particular attention to identifying and explaining the parton momentum density functions. Explain also why the factor $\frac{M_W^2}{M_W^2+Q^2}$ appears.

(d) The table below gives $\tilde{\sigma}$ as measured by the ZEUS experiment for $e^\pm p \to \bar{\nu}_e X$ at $Q^2 = 3000$ GeV^2. Given the relation $Q^2 = sxy$, discuss qualitatively the differences between the e^+p and e^-p reduced cross sections.

x	e^+p $\tilde{\sigma}$	e^-p $\tilde{\sigma}$
0.068	$0{\cdot}37 \pm 0{\cdot}04$	$0{\cdot}64 \pm 0{\cdot}04$
0.130	$0{\cdot}27 \pm 0{\cdot}04$	$0{\cdot}58 \pm 0{\cdot}05$
0.240	$0{\cdot}22 \pm 0{\cdot}03$	$0{\cdot}50 \pm 0{\cdot}04$

6. The production of a charged lepton pair l^+l^- in high-energy collisions between two hadrons is called the Drell-Yan process. In the lowest-order process of this type between hadrons A and B, quark q from one hadron annihilates with anti-quark $\bar{q}$ from the other hadron, producing a time-like photon that converts to a real lepton-antilepton pair.

(a) Draw a space-time diagram of this process.

(b) Show that $\hat{s}$, the centre-of-mass squared in the $q\bar{q}$ system, is given by the approximate expression $\hat{s} = x\bar{x}s$, where x and $\bar{x}$ are the fractional momenta of the q and $\bar{q}$ quarks, and s is the centre-of-mass energy squared in the AB system. Make clear any approximations made.

(c) The cross-section for annihilation of q and $\bar{q}$ (for the case in which the colour of the $\bar{q}$ is opposite to that of the q) is:

$$\hat{\sigma} = \frac{4\pi}{3}\frac{\alpha^2 Q_q^2}{\hat{s}},$$

where α is the fine-structure constant and Q_q is the charge of quark q in units of e. Explain the physical origin of this formula.

(d) In the simple quark model, the differential cross-section σ for $AB \to l^+l^-X$ is

$$\frac{d^2\sigma}{dxd\bar{x}} = \frac{1}{3}\sum_{flavours}\hat{\sigma}(\hat{s})[F_q^A(x)F_{\bar{q}}^B(\bar{x}) + F_{\bar{q}}^A(\bar{x})F_q^B(x)].$$

Explain the meaning of the structure functions $F_q^{A(B)}$ and $F_q^{B(A)}$ and the physical basis of the above expression.

(e) The carbon nucleus has an equal number of protons and neutrons and thus also an equal number of u and d quarks. Show that in the quark model, the ratio

$$r = \frac{\sigma(\pi^+ C \to \mu^+\mu^- X)}{\sigma(\pi^- C \to \mu^+\mu^- X)}$$

equals 1/4 when $\hat{s}/s$ approaches 1. What value does r have to be for small $\hat{s}/s$?

(f) What are the dominant background for Drell-Yan reactions? Hence explain which channels would be best for studying this process. What detector systems would be required for one of these channels and what parameters of the system would be important for separating signal from background?

7. past paper question.

In the simple quark-parton model the cross section for deep inelastic electron proton scattering is given by

$$\frac{\mathrm{d}^2\sigma}{\mathrm{d}x\mathrm{d}y} = \sum_i x f_i(x)\frac{2\pi\alpha^2 s}{Q^4}q_i^2\left[1 + (1-y)^2\right] \qquad \text{for } Q^2 \ll M_Z^2c^2, \tag{1}$$

where s is the square of the e-p centre-of-mass energy, Q^2 is the negative of the squared 4-momentum transfer between the electron and the proton, and y is a function of the scattering angle θ in the e-q centre-of-mass frame, $y = \frac{1}{2}(1 - \cos\theta)$.

(a) Justify qualitatively the form of the above expression, explaining the form of the dependence on y, s and α. What do the variable x, the parameter q_i and the function $f_i(x)$ represent in the quark-parton model? [10]

(b) What is meant by the term *Bjorken-scaling*? How does Quantum Chromodynamics modify the predictions of the quark-parton model? [3]

(c) Starting from equation (1), but restricting your model to u and d flavours only, show that the proton structure function F_2^{ep} may be written as

$$F_2^{ep} = \frac{4}{9}x[u(x) + \bar{u}(x)] + \frac{1}{9}x[d(x) + \bar{d}(x)],$$

and define the terms. If scattering is performed using a deuteron target how would this formula be modified? [4]

(d) Deep inelastic scattering can also be performed using neutrino probes. The quark-parton model expression for neutrino-proton scattering through the exchange of a W boson is given by

$$\frac{d^2\sigma}{dxdy} = \frac{sG_F^2}{\pi}\left[\sum_i xf_i(x) + (1-y)^2\sum_{\bar{i}} x\bar{f}_i(x)\right], \qquad \text{for } Q^2 \ll M_W^2c^2. \qquad (2)$$

Explain the form of this expression, paying particular attention to the y-dependence and the flavours entering the sums. How would the flavour structure be modified for neutrino-deuteron scattering? By comparing your expression to the general form

$$\frac{d^2\sigma}{dxdy}^{\nu D} = \frac{sG_F^2}{4\pi}\left(\frac{M_W^2}{M_W^2+Q^2}\right)^2\left[(1+(1-y)^2)F_2^{\nu D} + (1-(1-y)^2)xF_3^{\nu D}\right],$$

write down the quark-parton model prediction for the $F_2^{\nu\mathrm{D}}$ structure function and hence derive the relationship

$$F_2^{\mathrm{eD}} = \frac{5}{18}F_2^{\nu\mathrm{D}}.$$

[8]